

# Two-Loop QCD Anomalous Dimensions of Flavour-Changing Four-Quark Operators Within and Beyond the Standard Model

Andrzej J. Buras<sup>1</sup>, Mikołaj Misiak<sup>2,3</sup> and Jörg Urban<sup>1</sup>

<sup>1</sup>*Physik Department, Technische Universität München,  
 D-85748 Garching, Germany*

<sup>2</sup>*Theory Division, CERN, CH-1211 Geneva 23, Switzerland*

<sup>3</sup>*Institute of Theoretical Physics, Warsaw University,  
 Hoża 69, PL-00-681 Warsaw, Poland*

## Abstract

We calculate the two-loop QCD anomalous dimension matrix (ADM)  $(\hat{\gamma}^{(1)})_{\text{NDR}}$  in the NDR- $\overline{\text{MS}}$  scheme for all the flavour-changing four-quark dimension-six operators that are relevant in both the Standard Model and its extensions. Both current-current and penguin diagrams are included. Some of our NDR- $\overline{\text{MS}}$  results for  $\Delta F = 1$  operators overlap with the previous calculations, but several others have never been published before. In the case of  $\Delta F = 2$  operators, our results are compatible with the ones obtained by Ciuchini et al. in the Regularization-Independent renormalization scheme, but differ from their NDR- $\overline{\text{MS}}$  results. In order to explain the difference, we calculate the ADM of  $\Delta F = 2$  operators again, extracting it from the ADM of  $\Delta F = 1$  operators.

# 1 Introduction

Renormalization group short-distance QCD effects play an important role in the phenomenology of non-leptonic weak transitions of  $K$ -,  $D$ - and  $B$ -mesons. An essential ingredient in any renormalization group analysis is the anomalous dimension matrix (ADM), which describes the mixing of the relevant local four-quark operators under renormalization [1, 2].

The operators considered in the present paper have the form

$$\bar{\Psi}_1^\alpha \Gamma_A^k \Psi_2^\alpha \bar{\Psi}_3^\beta \Gamma_B^k \Psi_4^\beta, \quad \bar{\Psi}_1^\alpha \Gamma_A^k \Psi_2^\beta \bar{\Psi}_3^\beta \Gamma_B^k \Psi_4^\alpha, \quad (1.1)$$

where  $\alpha, \beta$  are colour indices and  $\Gamma_{A,B}^k$  are generic Dirac matrices given explicitly below. The subscripts  $i$  in  $\Psi_i$  are flavour indices. In the case of FCNC transitions with  $\Delta F = 2$ , such as neutral meson mixing, one has

$$\Psi_1 = \Psi_3, \quad \Psi_2 = \Psi_4. \quad (1.2)$$

Known examples are the operators  $(\bar{s}d)_{V-A}(\bar{s}d)_{V-A}$  and  $(\bar{b}d)_{V-A}(\bar{b}d)_{V-A}$  relevant in the Standard Model (SM) to  $K^0-\bar{K}^0$  and  $B_d^0-\bar{B}_d^0$  mixing, respectively.

Four-quark operators that occur in the SM calculations of flavour-changing processes do not form a complete set of all the dimension-six four-quark operators. Other operators need to be considered in many extensions of the SM, e.g. in the Supersymmetric Standard Model (SSM) (see e.g. ref. [3]). For instance, the SSM and SM predictions for  $K^0-\bar{K}^0$  and  $B_d^0-\bar{B}_d^0$  mixing can have similar precision only if the two-loop ADM for *all* the  $\Delta F = 2$  operators is known.

The main purpose of the present paper is a calculation of the two-loop ADM for all the dimension-six flavour-changing four-quark operators in the NDR- $\overline{\text{MS}}$  scheme ( $\overline{\text{MS}}$  scheme with fully anticommuting  $\gamma_5$ ). Our main findings are the NDR- $\overline{\text{MS}}$  anomalous dimensions of the operators with Dirac structures (cf. eq. (1.1)):

$$\Gamma_A^k \otimes \Gamma_B^k = (1 \pm \gamma_5) \otimes (1 \pm \gamma_5) \quad \text{and} \quad \Gamma_A^k \otimes \Gamma_B^k = [\sigma_{\mu\nu}(1 \pm \gamma_5)] \otimes [\sigma^{\mu\nu}(1 \pm \gamma_5)]. \quad (1.3)$$

For these operators, our two-loop results differ from the NDR- $\overline{\text{MS}}$  ones of Ciuchini et al. [4], but are compatible with their RI-scheme ADM. For all the other operators, no new calculation

is actually necessary — all the two-loop results can be extracted from the existing Standard Model ones.

Our paper is organized as follows. In section 2, we perform a direct calculation of the NDR- $\overline{\text{MS}}$ -scheme ADM of  $\Delta F = 2$  operators. This is a relatively straightforward computation, since all the methods are already known from similar SM calculations (see e.g. refs. [5]–[8]). The only novelty here is the introduction of evanescent operators that vanish by the Fierz identities.

In section 3, we compute the NDR- $\overline{\text{MS}}$  ADM for such  $\Delta F = 1$  operators, to which only the current–current diagrams are relevant. Some of the  $\Delta F = 1$  results have never been published before. The ones that are not new agree with the old SM calculations. The subject of section 4 are  $\Delta F = 1$  operators containing one quark–antiquark pair of the same flavour. We identify the operators to which the so-called penguin diagrams are relevant, and give the corresponding anomalous dimensions.

In section 5, we derive the matrix  $\Delta\hat{r}$  necessary for transforming the Wilson coefficients from the NDR- $\overline{\text{MS}}$  to the RI scheme (originally called the MOM scheme) that is more useful for non-perturbative calculations of hadronic matrix elements [9].

Section 6 is devoted to performing a consistency check of our  $\Delta F = 1$  and  $\Delta F = 2$  results. The current–current ADM of  $\Delta F = 1$  operators is transformed there to such an operator basis, in which the  $\Delta F = 2$  results can be easily read off. This calculation serves also as a preparation for the comparison with Ciuchini et al. [4]. Comparison with this article and other existing literature is the subject of section 7. We conclude in section 8.

In appendix A, we list the evanescent operators relevant to the  $\Delta F = 2$  calculation. In appendix B, an analogous list for the  $\Delta F = 1$  case is presented. Appendix C contains additional evanescent operators that become important *only* when one wants to derive the  $\Delta F = 2$  results from the  $\Delta F = 1$  ones, as in section 6. Appendix D is devoted to recalling and generalizing the notion of “Greek projections”. Appendix E contains a list of separate contributions from different diagrams to the one- and two-loop ADMs for  $\Delta F = 1$  operators with Dirac structures (1.3). Finally, in appendix F, we outline our determination of two-loop mixing via penguin diagrams that involves beyond-SM operators.

## 2 Direct calculation of the ADM in the $\Delta F = 2$ case

For definiteness, we shall consider here operators responsible for the  $K^0-\bar{K}^0$  mixing. There are 8 such operators of dimension 6. They can be split into 5 separate sectors, according to the chirality of the quark fields they contain. The operators belonging to the first three sectors (VLL, LR and SLL) read

$$\begin{aligned}
Q_1^{\text{VLL}} &= (\bar{s}^\alpha \gamma_\mu P_L d^\alpha)(\bar{s}^\beta \gamma^\mu P_L d^\beta), \\
Q_1^{\text{LR}} &= (\bar{s}^\alpha \gamma_\mu P_L d^\alpha)(\bar{s}^\beta \gamma^\mu P_R d^\beta), \\
Q_2^{\text{LR}} &= (\bar{s}^\alpha P_L d^\alpha)(\bar{s}^\beta P_R d^\beta), \\
Q_1^{\text{SLL}} &= (\bar{s}^\alpha P_L d^\alpha)(\bar{s}^\beta P_L d^\beta), \\
Q_2^{\text{SLL}} &= (\bar{s}^\alpha \sigma_{\mu\nu} P_L d^\alpha)(\bar{s}^\beta \sigma^{\mu\nu} P_L d^\beta),
\end{aligned} \tag{2.1}$$

where  $\sigma_{\mu\nu} = \frac{1}{2}[\gamma_\mu, \gamma_\nu]$  and  $P_{L,R} = \frac{1}{2}(1 \mp \gamma_5)$ . The operators belonging to the two remaining sectors (VRR and SRR) are obtained from  $Q_1^{\text{VLL}}$  and  $Q_i^{\text{SLL}}$  by interchanging  $P_L$  and  $P_R$ . Since QCD preserves chirality, there is no mixing between different sectors. Moreover, the ADMs in the VRR and SRR sectors are the same as in the VLL and SLL sectors, respectively. In the following, we shall consider only the VLL, LR and SLL sectors.

In dimensional regularization, the four-quark operators from eq. (2.1) mix at one loop into the evanescent operators listed in appendix A. Specifying these evanescent operators is necessary to make precise the definition of the NDR- $\overline{\text{MS}}$  scheme in the effective theory [5, 8, 10, 11]. An important novelty in the present case (when compared to  $\Delta F = 1$  calculations) is the necessity of introducing evanescent operators that vanish in 4 dimensions by the Fierz identities. The Fierz identities cannot be analytically continued to  $D$  dimensions. Therefore, they have to be treated in dimensional regularization in the same manner as the identity

$$\gamma_\mu \gamma_\nu \gamma_\rho = g_{\mu\nu} \gamma_\rho + g_{\nu\rho} \gamma_\mu - g_{\mu\rho} \gamma_\nu + i \epsilon_{\alpha\mu\nu\rho} \gamma^\alpha \gamma_5, \tag{2.2}$$

i.e. appropriate evanescent operators have to be introduced.

As an example, consider the operators  $Q_1^{\text{SLL}}$  and  $Q_2^{\text{SLL}}$ . When these operators are inserted into one- and two-loop diagrams, the operators

$$\tilde{Q}_1^{\text{SLL}} = (\bar{s}^\alpha P_L d^\beta)(\bar{s}^\beta P_L d^\alpha), \quad (2.3)$$

$$\tilde{Q}_2^{\text{SLL}} = (\bar{s}^\alpha \sigma_{\mu\nu} P_L d^\beta)(\bar{s}^\beta \sigma^{\mu\nu} P_L d^\alpha) \quad (2.4)$$

are generated. In 4 dimensions these operators can be expressed through  $Q_1^{\text{SLL}}$  and  $Q_2^{\text{SLL}}$  by using the Fierz identities

$$\begin{aligned} (P_L)_{ij}(P_L)_{kl} &= \frac{1}{2}(P_L)_{il}(P_L)_{kj} - \frac{1}{8}(\sigma_{\mu\nu} P_L)_{il}(\sigma^{\mu\nu} P_L)_{kj}, \\ (\sigma_{\mu\nu} P_L)_{ij}(\sigma^{\mu\nu} P_L)_{kl} &= -6(P_L)_{il}(P_L)_{kj} - \frac{1}{2}(\sigma_{\mu\nu} P_L)_{il}(\sigma^{\mu\nu} P_L)_{kj}, \end{aligned} \quad (2.5)$$

which give

$$\tilde{Q}_1^{\text{SLL}} \stackrel{D=4}{=} -\frac{1}{2} Q_1^{\text{SLL}} + \frac{1}{8} Q_2^{\text{SLL}}, \quad (2.6)$$

$$\tilde{Q}_2^{\text{SLL}} \stackrel{D=4}{=} 6 Q_1^{\text{SLL}} + \frac{1}{2} Q_2^{\text{SLL}}. \quad (2.7)$$

These relations can be used in the calculation of one-loop ADM. In the case of two-loop calculations, in the NDR- $\overline{\text{MS}}$  scheme, where Dirac algebra has to be performed in  $D \neq 4$  dimensions, these relations have to be generalized to

$$\tilde{Q}_1^{\text{SLL}} = -\frac{1}{2} Q_1^{\text{SLL}} + \frac{1}{8} Q_2^{\text{SLL}} + E_1^{\text{SLL}}, \quad (2.8)$$

$$\tilde{Q}_2^{\text{SLL}} = 6 Q_1^{\text{SLL}} + \frac{1}{2} Q_2^{\text{SLL}} + E_2^{\text{SLL}}. \quad (2.9)$$

Here,  $E_1^{\text{SLL}}$  and  $E_2^{\text{SLL}}$  are the evanescent operators that vanish in 4 dimensions by Fierz identities. They are simply defined by (2.8) and (2.9) and are given in appendix A.

The effective Lagrangian can be written separately for each sector. It takes the form

$$\mathcal{L}_{eff} = -\frac{G_F^2 M_W^2}{4\pi^2} (V_{ts}^* V_{td})^2 Z_q^2 \sum_i C_i(\mu) [Q_i + (\text{counterterms})_i], \quad (2.10)$$

where  $Z_q$  is the quark wave-function renormalization constant.

The coefficients  $C_i(\mu)$  satisfy the Renormalization Group Equation (RGE)

$$\mu \frac{d}{d\mu} \vec{C}(\mu) = \hat{\gamma}(\mu)^T \vec{C}(\mu) \quad (2.11)$$

governed by the ADM  $\hat{\gamma}(\mu)$  that has the following perturbative expansion:

$$\hat{\gamma}(\mu) = \frac{\alpha_s(\mu)}{4\pi} \hat{\gamma}^{(0)} + \frac{\alpha_s^2(\mu)}{(4\pi)^2} \hat{\gamma}^{(1)} + \mathcal{O}(\alpha_s^3). \quad (2.12)$$

The ADM in the MS or  $\overline{\text{MS}}$  scheme is found from one- and two-loop counterterms in the effective theory, according to the following relations (equivalent to eqs. (4.26)–(4.37) of ref. [5]):

$$\hat{\gamma}^{(0)} = 2\hat{a}^{11}, \quad (2.13)$$

$$\hat{\gamma}^{(1)} = 4\hat{a}^{12} - 2\hat{b}\hat{c}. \quad (2.14)$$

The matrices  $\hat{a}^{11}$ ,  $\hat{a}^{12}$  and  $\hat{b}$  in the above equations parametrize the MS-scheme counterterms in eq. (2.10) (for  $D = 4 - 2\epsilon$ )

$$\begin{aligned} (\text{counterterms})_i &= \frac{\alpha_s}{4\pi\epsilon} \left[ \sum_k a_{ik}^{11} Q_k + \sum_k b_{ik} E_k \right] + \frac{\alpha_s^2}{(4\pi)^2} \sum_k \left( \frac{1}{\epsilon^2} a_{ik}^{22} + \frac{1}{\epsilon} a_{ik}^{12} \right) Q_k \\ &+ (\text{two-loop evanescent counterterms}) + \mathcal{O}(\alpha_s^3). \end{aligned} \quad (2.15)$$

The matrix  $\hat{c}$  is recovered from one-loop matrix elements of the evanescent operators. Let us denote by  $\langle E_k \rangle_{1\text{loop}}$  the one-loop  $K^0\text{--}\bar{K}^0$  amplitude with an insertion of some evanescent operator  $E_k$ . The pole part of such an amplitude is proportional to some linear combination of tree-level matrix elements of evanescent operators. The remaining part in the limit  $D \rightarrow 4$  can be expressed by tree-level matrix elements of the physical operators  $Q_i$ . The finite coefficients of these matrix elements define the matrix  $\hat{c}$  as follows:

$$\langle E_k \rangle_{1\text{loop}} = -\frac{1}{\epsilon} \left[ \sum_j d_{kj} \langle E_j \rangle_{\text{tree}} + \sum_j e_{kj} \langle F_j \rangle_{\text{tree}} \right] - \sum_i c_{ki} \langle Q_i \rangle_{\text{tree}} + \mathcal{O}(\epsilon). \quad (2.16)$$

Here,  $F_j$  stand for such evanescent operators that are not necessary as counterterms for the one-loop Green functions with insertions of the physical operators  $Q_i$ . The matrices  $\hat{c}$  and  $\hat{a}^{12}$  depend on the structure of  $F_j$ , but  $\hat{\gamma}^{(1)}$  does not.

The matrices  $\hat{\gamma}^{(0)} = 2\hat{a}^{11}$ ,  $\hat{b}$  and  $\hat{c}$  in each sector are found from the one-loop  $d\bar{s} \rightarrow s\bar{d}$  diagrams presented in fig. 1 with insertions of the physical operators  $Q_i$ , as well as the evanescent operators  $E_k$ . We calculate only the ‘‘annihilation-type’’ diagrams, i.e. we drop all the diagrams where fermion lines connect the incoming and outgoing particles. Dropping such diagrams

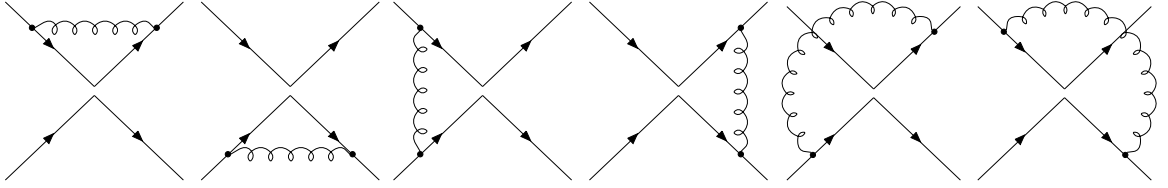


Figure 1: One-loop diagrams

consistently at the tree level, at one loop and (later) at two loops does not alter the final results for the renormalization constants.

All the one- and two-loop diagrams considered in the present article are calculated using two different methods. In both of them, a covariant gauge-fixing term

$$\mathcal{L}_{gf} = -\frac{1}{2\lambda}(\partial^\mu G_\mu^a)(\partial^\nu G_\nu^a) \quad (2.17)$$

is used, and the physical masses are set to zero. In the first method, the external quarks are assumed to have momentum  $\pm p$ . In the second method, the external momenta are set to zero, but a common mass parameter is introduced in all the propagator denominators as IR regulator [12]. The two methods give the same results for the  $\overline{\text{MS}}$  renormalization constants. The ADMs calculated from these renormalization constants with the help of eqs. (2.13) and (2.14) are independent of the gauge-fixing parameter  $\lambda$ .

We begin with presenting the ADM in the SLL sector, because in this very sector our results are going to differ (at two loops) from those of ref. [4]. The matrices  $\hat{\gamma}^{(0)\text{SLL}}$  and  $\hat{b}^{\text{SLL}}$  are found to be the following:

$$\hat{\gamma}^{(0)\text{SLL}} = \begin{pmatrix} -6N + 6 + \frac{6}{N} & \frac{1}{2} - \frac{1}{N} \\ -24 - \frac{48}{N} & 2N + 6 - \frac{2}{N} \end{pmatrix}, \quad (2.18)$$

$$\hat{b}^{\text{SLL}} = \begin{pmatrix} 0 & \frac{1}{2} & 0 & 0 \\ -8 & -8 & -\frac{1}{2N} & \frac{1}{2} \end{pmatrix}, \quad (2.19)$$

where  $N$  stands for the number of colours.

In order to find the matrix  $\hat{a}^{12}$ , we need to calculate two-loop diagrams obtained from the ones in fig. 1 by including one-loop corrections on the gluon lines or adding another gluon that couples to the open quark lines. Of course, one-loop diagrams with counterterm insertions

need to be included, too. All the two-loop diagrams and the corresponding colour factors are the same as in fig. 2 and table 2 of ref. [5]. However, in the present article, we also consider additional Dirac structures (1.3) in the four-quark vertices.

Inserting the calculated matrix  $\hat{a}^{12}$  into eq. (2.14), we obtain the two-loop ADM. Its entries are found to be the following:

$$\begin{aligned}
\gamma_{11}^{(1)\text{SLL}} &= -\frac{203}{6}N^2 + \frac{107}{3}N + \frac{136}{3} - \frac{12}{N} - \frac{107}{2N^2} + \frac{10}{3}Nf - \frac{2}{3}f - \frac{10}{3N}f, \\
\gamma_{12}^{(1)\text{SLL}} &= -\frac{1}{36}N - \frac{31}{9} + \frac{9}{N} - \frac{4}{N^2} - \frac{1}{18}f + \frac{1}{9N}f, \\
\gamma_{21}^{(1)\text{SLL}} &= -\frac{364}{3}N - \frac{704}{3} - \frac{208}{N} - \frac{320}{N^2} + \frac{136}{3}f + \frac{176}{3N}f, \\
\gamma_{22}^{(1)\text{SLL}} &= \frac{343}{18}N^2 + 21N - \frac{188}{9} + \frac{44}{N} + \frac{21}{2N^2} - \frac{26}{9}Nf - 6f + \frac{2}{9N}f,
\end{aligned} \tag{2.20}$$

where  $f$  stands for the number of active flavours. The above equation is one of the main results of the present paper.

Proceeding analogously in the VLL sector, we reproduce the well-known results for the one- and two-loop anomalous dimensions of the operator  $Q_1^{\text{VLL}}$  [13]:

$$\begin{aligned}
\gamma^{(0)\text{VLL}} &= 6 - \frac{6}{N}, \\
\gamma^{(1)\text{VLL}} &= -\frac{19}{6}N - \frac{22}{3} + \frac{39}{N} - \frac{57}{2N^2} + \frac{2}{3}f - \frac{2}{3N}f.
\end{aligned} \tag{2.21}$$

The matrix  $\hat{b}$  in the VLL sector reads

$$\hat{b}^{\text{VLL}} = \begin{pmatrix} -5 & -\frac{1}{2N} & \frac{1}{2} \end{pmatrix}. \tag{2.22}$$

Finally, our results for the LR sector read

$$\hat{\gamma}^{(0)\text{LR}} = \begin{pmatrix} \frac{6}{N} & 12 \\ 0 & -6N + \frac{6}{N} \end{pmatrix}, \tag{2.23}$$

$$\hat{\gamma}^{(1)\text{LR}} = \begin{pmatrix} \frac{137}{6} + \frac{15}{2N^2} - \frac{22}{3N}f & \frac{200}{3}N - \frac{6}{N} - \frac{44}{3}f \\ \frac{71}{4}N + \frac{9}{N} - 2f & -\frac{203}{6}N^2 + \frac{479}{6} + \frac{15}{2N^2} + \frac{10}{3}Nf - \frac{22}{3N}f \end{pmatrix}, \tag{2.24}$$

$$\hat{b}^{\text{LR}} = \begin{pmatrix} 0 & -5 & -\frac{1}{2N} & \frac{1}{2} & 0 & 0 \\ 0 & 0 & 0 & 0 & -\frac{1}{2N} & \frac{1}{2} \end{pmatrix}. \tag{2.25}$$

As mentioned in the introduction, all the comparisons with existing literature are relegated to section 7.



### 3 Current–current contributions to the ADM of $\Delta F = 1$ operators

In the present section, we evaluate contributions from the current–current diagrams to the ADM of  $\Delta F = 1$  operators. For this purpose, we choose the operators in such a manner that all the four flavours they contain are different:  $\bar{s}$ ,  $d$ ,  $\bar{u}$ ,  $c$ . In such a case, the only possible diagrams are the current–current ones.

Twenty linearly independent operators can be built out of four different quark fields. They can be split into 8 separate sectors, between which there is no mixing. The operators belonging to the first four sectors (VLL, VLR, SLR and SLL) read

$$\begin{aligned}
Q_1^{\text{VLL}} &= (\bar{s}^\alpha \gamma_\mu P_L d^\beta)(\bar{u}^\beta \gamma^\mu P_L c^\alpha) = \tilde{Q}_{V_L V_L}, \\
Q_2^{\text{VLL}} &= (\bar{s}^\alpha \gamma_\mu P_L d^\alpha)(\bar{u}^\beta \gamma^\mu P_L c^\beta) = Q_{V_L V_L}, \\
Q_1^{\text{VLR}} &= (\bar{s}^\alpha \gamma_\mu P_L d^\beta)(\bar{u}^\beta \gamma^\mu P_R c^\alpha) = \tilde{Q}_{V_L V_R}, \\
Q_2^{\text{VLR}} &= (\bar{s}^\alpha \gamma_\mu P_L d^\alpha)(\bar{u}^\beta \gamma^\mu P_R c^\beta) = Q_{V_L V_R}, \\
Q_1^{\text{SLR}} &= (\bar{s}^\alpha P_L d^\beta)(\bar{u}^\beta P_R c^\alpha) = \tilde{Q}_{LR}, \\
Q_2^{\text{SLR}} &= (\bar{s}^\alpha P_L d^\alpha)(\bar{u}^\beta P_R c^\beta) = Q_{LR}, \\
Q_1^{\text{SLL}} &= (\bar{s}^\alpha P_L d^\beta)(\bar{u}^\beta P_L c^\alpha) = \tilde{Q}_{LL}, \\
Q_2^{\text{SLL}} &= (\bar{s}^\alpha P_L d^\alpha)(\bar{u}^\beta P_L c^\beta) = Q_{LL}, \\
Q_3^{\text{SLL}} &= (\bar{s}^\alpha \sigma_{\mu\nu} P_L d^\beta)(\bar{u}^\beta \sigma^{\mu\nu} P_L c^\alpha) = \tilde{Q}_{T_L T_L}, \\
Q_4^{\text{SLL}} &= (\bar{s}^\alpha \sigma_{\mu\nu} P_L d^\alpha)(\bar{u}^\beta \sigma^{\mu\nu} P_L c^\beta) = Q_{T_L T_L},
\end{aligned} \tag{3.1}$$

where on the r.h.s. we have shown the notation of ref. [4].

The operators belonging to the four remaining sectors (VRR, VRL, SRL and SRR) are obtained from the above by interchanging  $P_L$  and  $P_R$ . Obviously, it is sufficient to calculate the ADMs only for the VLL, VLR, SLR and SLL sectors. The “mirror” operators in the VRR, VRL, SRL and SRR sectors will have exactly the same properties under QCD renormalization.

The evanescent operators for the VLL, VLR, SLR and SLL sectors are listed in appendix B. Calculation of the renormalization constants and the ADMs proceeds along the same lines as in the previous section. The relevant divergences in one- and two-loop diagrams in the cases of VLL, VLR and SLR sectors are given in refs. [5] and [6]. For completeness we give in appendix E the corresponding results for the SLL sector. These have not been published so far in the NDR- $\overline{\text{MS}}$  scheme.

Our final results for the  $\Delta F = 1$  ADMs are as follows:

$$\hat{\gamma}^{(0)\text{VLL}} = \begin{pmatrix} -\frac{6}{N} & 6 \\ 6 & -\frac{6}{N} \end{pmatrix}, \quad (3.2)$$

$$\hat{\gamma}^{(1)\text{VLL}} = \begin{pmatrix} -\frac{22}{3} - \frac{57}{2N^2} - \frac{2}{3N}f & -\frac{19}{6}N + \frac{39}{N} + \frac{2}{3}f \\ -\frac{19}{6}N + \frac{39}{N} + \frac{2}{3}f & -\frac{22}{3} - \frac{57}{2N^2} - \frac{2}{3N}f \end{pmatrix}, \quad (3.3)$$

$$\hat{\gamma}^{(0)\text{VLR}} = \begin{pmatrix} -6N + \frac{6}{N} & 0 \\ -6 & \frac{6}{N} \end{pmatrix}, \quad (3.4)$$

$$\hat{\gamma}^{(1)\text{VLR}} = \begin{pmatrix} -\frac{203}{6}N^2 + \frac{479}{6} + \frac{15}{2N^2} + \frac{10}{3}Nf - \frac{22}{3N}f & -\frac{71}{2}N - \frac{18}{N} + 4f \\ -\frac{100}{3}N + \frac{3}{N} + \frac{22}{3}f & \frac{137}{6} + \frac{15}{2N^2} - \frac{22}{3N}f \end{pmatrix}, \quad (3.5)$$

$$\hat{\gamma}^{(0)\text{SLR}} = \begin{pmatrix} \frac{6}{N} & -6 \\ 0 & -6N + \frac{6}{N} \end{pmatrix}, \quad (3.6)$$

$$\hat{\gamma}^{(1)\text{SLR}} = \begin{pmatrix} \frac{137}{6} + \frac{15}{2N^2} - \frac{22}{3N}f & -\frac{100}{3}N + \frac{3}{N} + \frac{22}{3}f \\ -\frac{71}{2}N - \frac{18}{N} + 4f & -\frac{203}{6}N^2 + \frac{479}{6} + \frac{15}{2N^2} + \frac{10}{3}Nf - \frac{22}{3N}f \end{pmatrix}, \quad (3.7)$$

$$\hat{\gamma}^{(0)\text{SLL}} = \begin{pmatrix} \frac{6}{N} & -6 & \frac{N}{2} - \frac{1}{N} & \frac{1}{2} \\ 0 & -6N + \frac{6}{N} & 1 & -\frac{1}{N} \\ -\frac{48}{N} + 24N & 24 & -\frac{2}{N} - 4N & 6 \\ 48 & -\frac{48}{N} & 0 & 2N - \frac{2}{N} \end{pmatrix}, \quad (3.8)$$

$$\gamma_{11}^{(1)\text{SLL}} = -\frac{N^2}{2} + \frac{148}{3} - \frac{107}{2N^2} - 2Nf - \frac{10}{3N}f,$$

$$\gamma_{12}^{(1)\text{SLL}} = -\frac{178}{3}N + \frac{64}{N} + \frac{16}{3}f,$$

$$\gamma_{13}^{(1)\text{SLL}} = \frac{107}{36}N^2 - \frac{71}{18} - \frac{4}{N^2} - \frac{1}{18}Nf + \frac{f}{9N},$$

$$\gamma_{14}^{(1)\text{SLL}} = -\frac{109}{36}N + \frac{8}{N} - \frac{f}{18},$$

$$\gamma_{21}^{(1)\text{SLL}} = -26N + \frac{104}{N},$$

$$\gamma_{22}^{(1)\text{SLL}} = -\frac{203}{6}N^2 + \frac{28}{3} - \frac{107}{2N^2} + \frac{10}{3}Nf - \frac{10}{3N}f,$$

$$\begin{aligned}
\gamma_{23}^{(1)\text{SLL}} &= \frac{89}{18}N + \frac{2}{N} - \frac{1}{9}f, \\
\gamma_{24}^{(1)\text{SLL}} &= -\frac{53}{18} - \frac{4}{N^2} + \frac{1}{9N}f, \\
\gamma_{31}^{(1)\text{SLL}} &= \frac{676}{3}N^2 - \frac{1880}{3} - \frac{320}{N^2} - \frac{88}{3}Nf + \frac{176}{3N}f, \\
\gamma_{32}^{(1)\text{SLL}} &= \frac{820}{3}N + \frac{448}{N} - \frac{88}{3}f, \\
\gamma_{33}^{(1)\text{SLL}} &= -\frac{257}{18}N^2 - \frac{116}{9} + \frac{21}{2N^2} + \frac{22}{9}Nf + \frac{2}{9N}f, \\
\gamma_{34}^{(1)\text{SLL}} &= \frac{50}{3}N - \frac{8}{3}f, \\
\gamma_{41}^{(1)\text{SLL}} &= \frac{488}{3}N + \frac{416}{N} - \frac{176}{3}f, \\
\gamma_{42}^{(1)\text{SLL}} &= -\frac{776}{3} - \frac{320}{N^2} + \frac{176}{3N}f, \\
\gamma_{43}^{(1)\text{SLL}} &= \frac{22}{3}N - \frac{40}{N} + \frac{8}{3}f, \\
\gamma_{44}^{(1)\text{SLL}} &= \frac{343}{18}N^2 + \frac{28}{9} + \frac{21}{2N^2} - \frac{26}{9}Nf + \frac{2}{9N}f.
\end{aligned} \tag{3.9}$$

Equation (3.9) is one of the main results of this work.

The careful reader has already noticed that the following equalities hold up to  $\mathcal{O}(\alpha_s^2)$ :

$$\begin{aligned}
\gamma_{11}^{\text{VLL}} &= \gamma_{22}^{\text{VLL}}, & \gamma_{12}^{\text{VLL}} &= \gamma_{21}^{\text{VLL}}, & \gamma_{11}^{\text{VLR}} &= \gamma_{22}^{\text{SLR}}, \\
\gamma_{22}^{\text{VLR}} &= \gamma_{11}^{\text{SLR}}, & \gamma_{12}^{\text{VLR}} &= \gamma_{21}^{\text{SLR}}, & \gamma_{21}^{\text{VLR}} &= \gamma_{12}^{\text{SLR}}.
\end{aligned} \tag{3.10}$$

At one loop, these equalities are a consequence of the Fierz identities

$$(\gamma_\mu P_L)_{ij}(\gamma^\mu P_L)_{kl} = -(\gamma_\mu P_L)_{il}(\gamma^\mu P_L)_{kj}, \tag{3.11}$$

$$(\gamma_\mu P_L)_{ij}(\gamma^\mu P_R)_{kl} = 2(P_R)_{il}(P_L)_{kj}, \tag{3.12}$$

as well as the flavour- and chirality-blind character of QCD interactions. Since the Fierz identities are satisfied in four spacetime dimensions only, the relations (3.10) could be potentially broken at two loops in the NDR- $\overline{\text{MS}}$  scheme. Surprisingly, they are not.<sup>1</sup>

On the contrary, analogous relations *are* broken at two loops in the SLL sector. Because of the Fierz relations (2.5), the one-loop matrix  $\hat{\gamma}^{(0)\text{SLL}}$  must satisfy the following identity (cf. eqs. (9) and (10) of ref. [4]):

$$\hat{\gamma}^{(0)\text{SLL}} = \hat{\mathcal{F}}\hat{\gamma}^{(0)\text{SLL}}\hat{\mathcal{F}} \tag{3.13}$$

---

<sup>1</sup>In section 4, where the penguin diagrams are considered, no invariance under Fierz rearrangement is observed at two loops for the operators with VLL Dirac structure. A detailed discussion of this fact can be found in ref. [6].

with

$$\hat{\mathcal{F}} = \begin{pmatrix} 0 & -\frac{1}{2} & 0 & \frac{1}{8} \\ -\frac{1}{2} & 0 & \frac{1}{8} & 0 \\ 0 & 6 & 0 & \frac{1}{2} \\ 6 & 0 & \frac{1}{2} & 0 \end{pmatrix}. \quad (3.14)$$

No similar relation holds for  $\hat{\gamma}^{(1)\text{SLL}}$  in the NDR- $\overline{\text{MS}}$  scheme. As it has already been said, this is not surprising, because the Fierz identities are not true in  $D \neq 4$  dimensions.

It is unclear to us whether the symmetries (3.10) for the VLL, VLR and SLR sectors are preserved at two loops in the NDR- $\overline{\text{MS}}$  scheme only by coincidence, or if there is some reason beyond this. As we shall see in section 6, this question is related to the properties of one-loop matrix elements of certain evanescent operators.

## 4 Penguin contributions to the ADM of $\Delta F = 1$ operators

In the present section, we shall describe additional contributions to the ADM of  $\Delta F = 1$  operators that are due to penguin diagrams. Such contributions may arise only when the operators contain one quark-antiquark pair of the same flavour.

For definiteness, let us consider  $\Delta S = 1$  operators. In the SM analysis of ref. [6], 10 such operators were considered<sup>2</sup>

$$\begin{aligned} Q_1 &= (\bar{s}^\alpha \gamma_\mu P_L u^\beta)(\bar{u}^\beta \gamma^\mu P_L d^\alpha), \\ Q_2 &= (\bar{s}^\alpha \gamma_\mu P_L u^\alpha)(\bar{u}^\beta \gamma^\mu P_L d^\beta), \\ Q_3 &= (\bar{s}^\alpha \gamma_\mu P_L d^\alpha) \sum_q (\bar{q}^\beta \gamma^\mu P_L q^\beta), \\ Q_4 &= (\bar{s}^\alpha \gamma_\mu P_L d^\beta) \sum_q (\bar{q}^\beta \gamma^\mu P_L q^\alpha), \\ Q_5 &= (\bar{s}^\alpha \gamma_\mu P_L d^\alpha) \sum_q (\bar{q}^\beta \gamma^\mu P_R q^\beta), \\ Q_6 &= (\bar{s}^\alpha \gamma_\mu P_L d^\beta) \sum_q (\bar{q}^\beta \gamma^\mu P_R q^\alpha), \end{aligned}$$

---

<sup>2</sup>Our operators here differ from the ones in ref. [6] by a global normalization factor of 4. Of course, it does not affect their ADM. The factor of 4 can be absorbed into the global normalization factor of the effective Lagrangian, as the first ratio on the r.h.s. of eq. (2.10). In this case, the Wilson coefficients of our operators are exactly the same as those in ref. [6].

$$\begin{aligned}
Q_7 &= \frac{3}{2}(\bar{s}^\alpha \gamma_\mu P_L d^\alpha) \sum_q e_q(\bar{q}^\beta \gamma^\mu P_R q^\beta), \\
Q_8 &= \frac{3}{2}(\bar{s}^\alpha \gamma_\mu P_L d^\beta) \sum_q e_q(\bar{q}^\beta \gamma^\mu P_R q^\alpha), \\
Q_9 &= \frac{3}{2}(\bar{s}^\alpha \gamma_\mu P_L d^\alpha) \sum_q e_q(\bar{q}^\beta \gamma^\mu P_L q^\beta), \\
Q_{10} &= \frac{3}{2}(\bar{s}^\alpha \gamma_\mu P_L d^\beta) \sum_q e_q(\bar{q}^\beta \gamma^\mu P_L q^\alpha). \tag{4.1}
\end{aligned}$$

Their one- and two-loop ADMs, including current–current and penguin diagrams, can be found in appendices A and B of ref. [6]. They were also obtained in ref. [7]. The same results hold for the mirror copies of the SM operators, i.e. for the operators obtained from the ones in eq. (4.1) by  $P_L \leftrightarrow P_R$  interchange.

Beyond SM, new linearly independent operators appear. Their Dirac structures are as in eq. (3.1). Our aim is to find a minimal set of linearly independent new operators. In the process of identifying these operators, we shall use four-dimensional Dirac algebra, including the Fierz relations (2.5), (3.11) and (3.12). It turns out that only 3 additional operators (and their mirror copies) undergo mixing via penguin diagrams into other four-quark operators in eq. (4.1). These are

$$\begin{aligned}
Q_{11} &= (\bar{s}^\alpha \gamma_\mu P_L d^\alpha) \left[ (\bar{d}^\beta \gamma^\mu P_L d^\beta) + (\bar{s}^\beta \gamma^\mu P_L s^\beta) \right], \\
Q_{12} &= (\bar{s}^\alpha \gamma_\mu P_L d^\beta) \left[ (\bar{d}^\beta \gamma^\mu P_R d^\alpha) + (\bar{s}^\beta \gamma^\mu P_R s^\alpha) \right], \\
Q_{13} &= (\bar{s}^\alpha \gamma_\mu P_L d^\alpha) \left[ (\bar{d}^\beta \gamma^\mu P_R d^\beta) + (\bar{s}^\beta \gamma^\mu P_R s^\beta) \right]. \tag{4.2}
\end{aligned}$$

The remaining elements of the operator basis can be chosen in such a manner that massless penguin diagrams with their insertions vanish. The first three of the remaining operators have the structure of  $Q_{11}$ , ...,  $Q_{13}$ , but with a relative minus sign between the two terms. The next two have the structure of  $Q_5$  and  $Q_6$ , but the sum over flavour-conserving currents is replaced by a difference between the analogous  $u$ -quark and  $c$ -quark currents. Their mirror copies have to be included, as well. Further operators have the SLL and SRR Dirac structures as in eq. (1.3), or they have the form

$$(\bar{s}^\alpha P_{L,R} d^\beta)(\bar{q}^\beta P_{R,L} q^\alpha), \tag{4.3}$$

$$(\bar{s}^\alpha P_{L,R} d^\alpha)(\bar{q}^\beta P_{R,L} q^\beta) \quad (4.4)$$

where  $q$  has flavour *different* from  $s$  and  $d$ . It is straightforward to convince oneself that we have not missed any linearly independent  $\Delta S = 1$  operator in the above considerations.

Massless penguin diagrams with insertions of the operators (1.3), (4.3) and (4.4) vanish, because

$$\text{Tr}(S_{\text{odd}} P_{L,R}) = 0 \quad \text{and} \quad P_{L,R} S_{\text{odd}} P_{L,R} = 0, \quad (4.5)$$

where  $S_{\text{odd}}$  is a product of an odd number of Dirac  $\gamma$ -matrices. For dimensional reasons, only massless penguin diagrams can cause mixing into other four-quark operators. This means that all the  $\Delta S = 1$  operators, except for  $Q_1, \dots, Q_{13}$  and their mirror copies, mix only due to current–current diagrams, i.e. their ADMs are identical to the ones we have already calculated in sections 2 and 3.

At the two-loop level, a complication arises because generally the Fierz relations could be broken in  $D \neq 4$  dimensions. Consequently, our use of these relations in the identification of linearly independent operators could be put in question. However, as we have already discussed in section 2 and will elaborate in section 5, this complication can be avoided by introducing appropriate evanescent operators that vanish in four dimensions by Fierz identities. This allows us to restrict the basis of new physical operators (undergoing penguin mixing) to the one in eq. (4.2), even at the two-loop level.

The introduction of evanescent operators that vanish in four dimensions by Fierz identities turns out to have no effect on the two-loop ADM in the case of the operators with VLR and SLR structures, because the Fierz identity (3.12) remains valid at two loops in the NDR- $\overline{\text{MS}}$  scheme, even if the penguin insertions are considered [6]. On the other hand, as pointed out in ref. [6], the Fierz identity (3.11) is broken at two loops in the NDR- $\overline{\text{MS}}$  scheme through penguin diagrams, although it remains valid for current–current diagrams. As a result, the mixing of the operator

$$Q'_{11} = (\bar{s}^\alpha \gamma_\mu P_L d^\beta) \left[ (\bar{d}^\beta \gamma^\mu P_L d^\alpha) + (\bar{s}^\beta \gamma^\mu P_L s^\alpha) \right] \quad (4.6)$$

with the operators in eq. (4.1), through penguin diagrams, differs from the one of  $Q_{11}$  at the two-loop level. This can be easily verified by using the results of ref. [6]. As  $Q'_{11} = Q_{11}$  in  $D = 4$  dimensions due to the Fierz identity (3.11),  $Q'_{11}$  was not included in the basis (4.2). By working with  $Q_{11}$  and the evanescent operator  $Q'_{11} - Q_{11}$ , the explicit appearance of  $Q'_{11}$  can be avoided at any number of loops, so that the basis (4.2) remains unchanged.

The above discussion implies that the only additional ADMs we need to find in the present section are:

- The  $3 \times 3$  matrix  $\hat{\gamma}_{cc}$  describing the mixing of  $Q_{11}, \dots, Q_{13}$  among themselves.
- The  $3 \times 4$  matrix  $\hat{\gamma}_p$  describing the mixing of  $Q_{11}, \dots, Q_{13}$  into  $Q_3, \dots, Q_6$  via penguin diagrams. (Only  $Q_3, \dots, Q_6$  are generated by massless QCD penguin diagrams with four-quark operator insertions.)

The matrix  $\hat{\gamma}_{cc}$  is given by current–current diagrams only. It takes the form

$$\hat{\gamma}_{cc} = \begin{pmatrix} \gamma_{\Delta F=2}^{\text{VLL}} & 0 \\ 0 & \hat{\gamma}_{\Delta F=1}^{\text{VLR}} \end{pmatrix} \quad (4.7)$$

with  $\gamma_{\Delta F=2}^{\text{VLL}}$  and  $\hat{\gamma}_{\Delta F=1}^{\text{VLR}}$  taken from eqs. (2.21), (3.2) and (3.3).

The matrix  $\hat{\gamma}_p = \hat{\gamma}_p^{(0)} + \frac{\alpha_s}{4\pi} \hat{\gamma}_p^{(1)} + \dots$  that originates from penguin diagrams can be easily extracted from sections 3.2 and 5.3 of ref. [6]. We find<sup>3</sup>

$$\hat{\gamma}_p^{(0)} = \left( \frac{4}{3}, \frac{4}{3}, 0 \right)^T \times \left( -\frac{1}{N}, 1, -\frac{1}{N}, 1 \right), \quad (4.8)$$

$$\hat{\gamma}_p^{(1)T} = \begin{pmatrix} 6N - \frac{64}{27} - \frac{4}{3N} + \frac{172}{27N^2} & -\frac{112}{27} - \frac{356}{27N^2} & -6N + \frac{40}{3N} \\ \frac{352}{27}N - \frac{14}{3} - \frac{460}{27N} & -\frac{32}{27}N + \frac{500}{27N} & -\frac{22}{3} \\ -6N - \frac{244}{27} + \frac{32}{3N} - \frac{188}{27N^2} & \frac{140}{27} + \frac{148}{27N^2} & 6N + \frac{4}{3N} \\ \frac{172}{27}N - \frac{14}{3} + \frac{260}{27N} & \frac{220}{27}N - \frac{508}{27N} & -\frac{22}{3} \end{pmatrix}. \quad (4.9)$$

The above discussion changes very little in the case of  $\Delta F = 1$  operators, in which  $F$  is the up-type flavour. Similarly to the  $\Delta S = 1$  case, all the contributions from penguin diagrams can be easily extracted from ref. [6].

---

<sup>3</sup>The four integers marked in red in eq. (4.9) have been corrected with respect to the first (v1) arXiv version of the current paper. They are now in agreement with ref. [23] where a mistake in our original determination of  $\hat{\gamma}_p^{(1)}$  was pointed out. In the current version of the article, we include an extra appendix F where our extraction of  $\hat{\gamma}_p^{(0)}$  and  $\hat{\gamma}_p^{(1)}$  from the results of ref. [6] is outlined.

## 5 Transformation of the Wilson coefficients to the RI scheme

The ADMs calculated in the present work are given in the NDR- $\overline{\text{MS}}$  scheme that is most convenient for perturbative calculations. However, after the Wilson coefficients are evolved with the help of RGE (2.11) down to a low energy scale, it might be necessary to transform them to another scheme that is more appropriate for non-perturbative calculations of hadronic matrix elements [9]. One such scheme is the so-called Regularization-Independent (RI) scheme (originally called the MOM scheme) used in ref. [4]. Below, we shall give relations between the NDR- $\overline{\text{MS}}$ -renormalized and RI-renormalized Wilson coefficients of all the operators considered in sections 2 and 3.

For completeness, we begin with the definition of the RI scheme. For the massless quark propagator, the renormalization condition can be written as

$$\frac{i}{4} \left[ \gamma^\rho \frac{\partial}{\partial p^\rho} S(p)_R^{-1} \right]_{p^2 = -\mu^2} = 1, \quad (5.1)$$

where  $\mu$  is the subtraction scale. A simple one-loop calculation is necessary to verify that the renormalized inverse propagator in the RI scheme reads

$$S(p)_R^{-1} = -i\not{p} \left[ 1 - \frac{\alpha_s}{4\pi} C_F \lambda \left( \frac{1}{2} - \ln \frac{-p^2}{\mu^2} \right) \right] + \mathcal{O}(\alpha_s^2), \quad (5.2)$$

where  $C_F = \frac{N^2-1}{2N}$  and  $\lambda$  is the gauge-fixing parameter (cf. eq. (2.17)). In dimensional regularization, the corresponding quark wave-function renormalization constant reads

$$Z_q^{\text{RI}} = 1 - \frac{\alpha_s}{4\pi} C_F \lambda \left( \frac{1}{\epsilon} - \gamma + \ln(4\pi) + \frac{1}{2} \right), \quad (5.3)$$

provided the subtraction scale  $\mu$  is identified with the standard  $\overline{\text{MS}}$  renormalization scale.

Conditions similar to eq. (5.1) are imposed on renormalized matrix elements of the operators (2.1) and (3.1) among four external quarks with the same momentum  $p$ . The quarks are assumed to be massless here. For the  $\Delta F = 2$  operators, such matrix elements have the following form

$$\begin{aligned} \langle Q_1^{\text{VLL}} \rangle_R &= A_{11}^{\text{VLL}}(p^2) \langle Q_1^{\text{VLL}} \rangle_{\text{tree}} + B_{11}^{\text{VLL}}(p^2) p^\mu p_\nu \langle (\bar{s}^\alpha \gamma_\mu P_L d^\alpha) (\bar{s}^\beta \gamma^\nu P_L d^\beta) \rangle_{\text{tree}}, \\ \langle Q_1^{\text{LR}} \rangle_R &= A_{11}^{\text{LR}}(p^2) \langle Q_1^{\text{LR}} \rangle_{\text{tree}} + B_{11}^{\text{LR}}(p^2) p^\mu p_\nu \langle (\bar{s}^\alpha \gamma_\mu P_L d^\alpha) (\bar{s}^\beta \gamma^\nu P_R d^\beta) \rangle_{\text{tree}} \end{aligned}$$



$$\begin{aligned}
& + A_{12}^{\text{LR}}(p^2) \langle Q_2^{\text{LR}} \rangle_{\text{tree}} + B_{12}^{\text{LR}}(p^2) p^\mu p_\nu \langle (\bar{s}^\alpha \sigma_{\mu\rho} P_L d^\alpha) (\bar{s}^\beta \sigma^{\nu\rho} P_R d^\beta) \rangle_{\text{tree}}, \\
\langle Q_2^{\text{LR}} \rangle_R & = A_{21}^{\text{LR}}(p^2) \langle Q_1^{\text{LR}} \rangle_{\text{tree}} + B_{21}^{\text{LR}}(p^2) p^\mu p_\nu \langle (\bar{s}^\alpha \gamma_\mu P_L d^\alpha) (\bar{s}^\beta \gamma^\nu P_R d^\beta) \rangle_{\text{tree}} \\
& + A_{22}^{\text{LR}}(p^2) \langle Q_2^{\text{LR}} \rangle_{\text{tree}} + B_{22}^{\text{LR}}(p^2) p^\mu p_\nu \langle (\bar{s}^\alpha \sigma_{\mu\rho} P_L d^\alpha) (\bar{s}^\beta \sigma^{\nu\rho} P_R d^\beta) \rangle_{\text{tree}}, \\
\langle Q_1^{\text{SLL}} \rangle_R & = A_{11}^{\text{SLL}}(p^2) \langle Q_1^{\text{SLL}} \rangle_{\text{tree}} + A_{12}^{\text{SLL}}(p^2) \langle Q_2^{\text{SLL}} \rangle_{\text{tree}}, \\
\langle Q_2^{\text{SLL}} \rangle_R & = A_{21}^{\text{SLL}}(p^2) \langle Q_1^{\text{SLL}} \rangle_{\text{tree}} + A_{22}^{\text{SLL}}(p^2) \langle Q_2^{\text{SLL}} \rangle_{\text{tree}}. \tag{5.4}
\end{aligned}$$

The formfactors  $B_{ij}(p^2)$  originate from UV-finite parts of Feynman diagrams and are scheme-independent. Note that in all the matrix elements multiplied by  $B_{ij}(p^2)$ , only colour-singlet quark currents occur. Colour-octet currents are removed from these terms with the help of the following Fierz identities (which are independent from the ones in eqs. (2.5), (3.11) and (3.12)):

$$(\not{p}P_L)_{ij}(\not{p}P_L)_{kl} = (\not{p}P_L)_{il}(\not{p}P_L)_{kj} - \frac{1}{2}p^2(\gamma_\mu P_L)_{il}(\gamma^\mu P_L)_{kj}, \tag{5.5}$$

$$(\not{p}P_L)_{ij}(\not{p}P_R)_{kl} = \frac{1}{2}p^\mu p_\nu (\sigma_{\mu\rho} P_R)_{il}(\sigma^{\nu\rho} P_L)_{kj} + \frac{1}{2}p^2(P_R)_{il}(P_L)_{kj}, \tag{5.6}$$

$$p^\mu p_\nu (\sigma_{\mu\rho} P_L)_{ij}(\sigma^{\nu\rho} P_R)_{kl} = 2(\not{p}P_R)_{il}(\not{p}P_L)_{kj} - \frac{1}{2}p^2(\gamma_\mu P_R)_{il}(\gamma^\mu P_L)_{kj}. \tag{5.7}$$

No  $B_{ij}$  formfactors occur in the SLL sector thanks to the four-dimensional identity

$$p^\mu p_\nu (\sigma_{\mu\rho} P_L)_{ij}(\sigma^{\nu\rho} P_L)_{kl} = \frac{1}{4}p^2(\sigma_{\mu\nu} P_L)_{ij}(\sigma^{\mu\nu} P_L)_{kl}. \tag{5.8}$$

The RI renormalization condition reads

$$A_{ij}(-\mu^2) - \omega\mu^2 B_{ij}(-\mu^2) = \delta_{ij}, \tag{5.9}$$

with

$$\omega = \begin{cases} \frac{1}{4} & \text{for } B_{11}^{\text{VLL}}, B_{11}^{\text{LR}} \text{ and } B_{21}^{\text{LR}}, \\ 0 & \text{otherwise.} \end{cases} \tag{5.10}$$

The renormalization condition (5.9) can be equivalently written as

$$A_{ij}^{\text{effective}}(p^2 = -\mu^2) = \delta_{ij}, \tag{5.11}$$

with  $A_{ij}^{\text{effective}}$  obtained from eqs. (5.4) by making the following *ad hoc* replacements

$$\begin{aligned}
(\not{p}P_L) \otimes (\not{p}P_{L,R}) & \rightarrow \frac{1}{4}p^2(\gamma_\mu P_L) \otimes (\gamma^\mu P_{L,R}), \\
p^\mu p_\nu (\sigma_{\mu\rho} P_{L,R}) \otimes (\sigma^{\nu\rho} P_{R,L}) & \rightarrow 0.
\end{aligned} \tag{5.12}$$

In the case of  $\Delta F = 1$  operators, the general structure of one-loop matrix elements is similar to that in eq. (5.4), but the number of formfactors is larger, because operators with colour-octet currents are now linearly independent. The matrix elements can be written as

$$\langle Q_i \rangle_R = A_{ij}^{\text{effective}}(p^2) \langle Q_j \rangle_{\text{tree}} + N_i, \quad (5.13)$$

where  $N_i$  vanish under the replacements (5.12). The RI renormalization condition then has the same form as in eq. (5.11).

In each of the sectors, the RI-renormalized Wilson coefficients can be obtained from the NDR- $\overline{\text{MS}}$ -renormalized ones with the help of the following relation

$$\vec{C}^{\text{RI}}(\mu) = \left( 1 - \frac{\alpha_s(\mu)}{4\pi} \Delta \hat{r}_{\overline{\text{MS}} \rightarrow \text{RI}}^T(\mu) \right) \vec{C}^{\overline{\text{MS}}}(\mu) + \mathcal{O}(\alpha_s^2), \quad (5.14)$$

where

$$[\Delta r_{\overline{\text{MS}} \rightarrow \text{RI}}(\mu)]_{ij} = \frac{4\pi}{\alpha_s(\mu)} [A_{ij}^{\text{RI}}(p^2) - A_{ij}^{\overline{\text{MS}}}(p^2)]. \quad (5.15)$$

The above relations can be easily derived from the fact that the renormalized matrix element of the whole effective Hamiltonian is scheme-independent, i.e.

$$\vec{C}^{\text{RI}}(\mu) \langle \vec{Q}(\mu, p^2) \rangle^{\text{RI}} = \vec{C}^{\overline{\text{MS}}}(\mu) \langle \vec{Q}(\mu, p^2) \rangle^{\overline{\text{MS}}}. \quad (5.16)$$

Again, the RI subtraction scale and the standard  $\overline{\text{MS}}$  renormalization scale have been tacitly identified. The external states must be the same in eq. (5.16). Consequently, the RI-scheme renormalization constant (5.3) must be used for external quark lines in  $A_{ij}^{\overline{\text{MS}}}(p^2)$  that enters into eq. (5.15).

The dependence on  $p^2$  and the explicit dependence on  $\mu$  cancels out in  $\Delta \hat{r}_{\overline{\text{MS}} \rightarrow \text{RI}}^T$  (5.15). However, one should not forget that this matrix depends on the gauge-fixing parameter  $\lambda$  that is, in turn,  $\mu$ -dependent.

Once the RI renormalization conditions have been specified, finding the explicit form of  $\Delta \hat{r}_{\overline{\text{MS}} \rightarrow \text{RI}}^T$  is only a matter of a straightforward one-loop computation. Our results for the  $\Delta F = 2$  operators are as follows:

$$\Delta r_{\overline{\text{MS}} \rightarrow \text{RI}}^{\text{VLL}} = 7 - \frac{7}{N} - 12 \ln 2 + \frac{12 \ln 2}{N} + \lambda \left( \frac{3}{2} - \frac{3}{2N} - 4 \ln 2 + \frac{4 \ln 2}{N} \right),$$

$$\begin{aligned}
\Delta \hat{r}_{\text{MS} \rightarrow \text{RI}}^{\text{LR}} &= \begin{pmatrix} \frac{2}{N} + \frac{2 \ln 2}{N} + \lambda \left( \frac{1}{2N} + \frac{2 \ln 2}{N} \right) & 4 + 4 \ln 2 + \lambda (1 + 4 \ln 2) \\ -1 + \ln 2 - \lambda \left( \frac{1}{2} - \ln 2 \right) & -4N + \frac{2}{N} + \frac{2 \ln 2}{N} - \lambda \left( \frac{3N}{2} - \frac{1}{2N} - \frac{2 \ln 2}{N} \right) \end{pmatrix}, \\
\left[ \Delta r_{\text{MS} \rightarrow \text{RI}}^{\text{SLL}} \right]_{11} &= -4N + 7 + \frac{5}{N} - 4 \ln 2 + \frac{2 \ln 2}{N} + \lambda \left( \frac{1}{2} + \frac{1}{2N} - \frac{3N}{2} + \frac{2 \ln 2}{N} \right), \\
\left[ \Delta r_{\text{MS} \rightarrow \text{RI}}^{\text{SLL}} \right]_{12} &= \frac{5}{12} - \frac{13}{12N} - \frac{2 \ln 2}{3} + \frac{5 \ln 2}{6N} + \lambda \left( \frac{5}{24} - \frac{1}{6N} - \frac{\ln 2}{3} + \frac{\ln 2}{6N} \right), \\
\left[ \Delta r_{\text{MS} \rightarrow \text{RI}}^{\text{SLL}} \right]_{21} &= 4 - \frac{12}{N} - 32 \ln 2 + \frac{40 \ln 2}{N} - \lambda \left( 2 + \frac{8}{N} + 16 \ln 2 - \frac{8 \ln 2}{N} \right), \\
\left[ \Delta r_{\text{MS} \rightarrow \text{RI}}^{\text{SLL}} \right]_{22} &= \frac{7}{3} - \frac{5}{3N} - \frac{28 \ln 2}{3} + \frac{26 \ln 2}{3N} + \lambda \left( \frac{N}{2} + \frac{7}{6} - \frac{5}{6N} - \frac{8 \ln 2}{3} + \frac{10 \ln 2}{3N} \right).
\end{aligned}$$

In the  $\Delta F = 1$  case, we find

$$\begin{aligned}
\Delta \hat{r}_{\text{MS} \rightarrow \text{RI}}^{\text{VLL}} &= \begin{pmatrix} -\frac{7}{N} + \frac{12 \ln 2}{N} - \lambda \left( \frac{3}{2N} - \frac{4 \ln 2}{N} \right) & 7 - 12 \ln 2 + \lambda \left( \frac{3}{2} - 4 \ln 2 \right) \\ 7 - 12 \ln 2 + \lambda \left( \frac{3}{2} - 4 \ln 2 \right) & -\frac{7}{N} + \frac{12 \ln 2}{N} - \lambda \left( \frac{3}{2N} - \frac{4 \ln 2}{N} \right) \end{pmatrix}, \\
\Delta \hat{r}_{\text{MS} \rightarrow \text{RI}}^{\text{VLR}} &= \begin{pmatrix} -4N + \frac{2}{N} + \frac{2 \ln 2}{N} - \lambda \left( \frac{3N}{2} - \frac{1}{2N} - \frac{2 \ln 2}{N} \right) & 2 - 2 \ln 2 + \lambda (1 - 2 \ln 2) \\ -2 - 2 \ln 2 - \lambda \left( \frac{1}{2} + 2 \ln 2 \right) & \frac{2}{N} + \frac{2 \ln 2}{N} + \lambda \left( \frac{1}{2N} + \frac{2 \ln 2}{N} \right) \end{pmatrix}, \\
\Delta \hat{r}_{\text{MS} \rightarrow \text{RI}}^{\text{SLR}} &= \begin{pmatrix} \frac{2}{N} + \frac{2 \ln 2}{N} + \lambda \left( \frac{1}{2N} + \frac{2 \ln 2}{N} \right) & -2 - 2 \ln 2 - \lambda \left( \frac{1}{2} + 2 \ln 2 \right) \\ 2 - 2 \ln 2 + \lambda (1 - 2 \ln 2) & -4N + \frac{2}{N} + \frac{2 \ln 2}{N} - \lambda \left( \frac{3N}{2} - \frac{1}{2N} - \frac{2 \ln 2}{N} \right) \end{pmatrix}, \\
\left[ \Delta r_{\text{MS} \rightarrow \text{RI}}^{\text{SLL}} \right]_{11} &= -\frac{3N}{2} + \frac{5}{N} + \frac{2 \ln 2}{N} + \lambda \left( \frac{1}{2N} + \frac{2 \ln 2}{N} \right), \\
\left[ \Delta r_{\text{MS} \rightarrow \text{RI}}^{\text{SLL}} \right]_{12} &= -\frac{7}{2} - 2 \ln 2 - \lambda \left( \frac{1}{2} + 2 \ln 2 \right), \\
\left[ \Delta r_{\text{MS} \rightarrow \text{RI}}^{\text{SLL}} \right]_{13} &= \frac{N}{2} - \frac{13}{12N} + \frac{5 \ln 2}{6N} + \lambda \left( \frac{N}{8} - \frac{1}{6N} + \frac{\ln 2}{6N} \right), \\
\left[ \Delta r_{\text{MS} \rightarrow \text{RI}}^{\text{SLL}} \right]_{14} &= \frac{7}{12} - \frac{5 \ln 2}{6} + \lambda \left( \frac{1}{24} - \frac{\ln 2}{6} \right), \\
\left[ \Delta r_{\text{MS} \rightarrow \text{RI}}^{\text{SLL}} \right]_{21} &= -1 - 2 \ln 2 + \lambda (1 - 2 \ln 2), \\
\left[ \Delta r_{\text{MS} \rightarrow \text{RI}}^{\text{SLL}} \right]_{22} &= -4N + \frac{5}{N} + \frac{2 \ln 2}{N} - \lambda \left( \frac{3N}{2} - \frac{1}{2N} - \frac{2 \ln 2}{N} \right), \\
\left[ \Delta r_{\text{MS} \rightarrow \text{RI}}^{\text{SLL}} \right]_{23} &= \frac{13}{12} - \frac{5 \ln 2}{6} + \lambda \left( \frac{1}{6} - \frac{\ln 2}{6} \right), \\
\left[ \Delta r_{\text{MS} \rightarrow \text{RI}}^{\text{SLL}} \right]_{24} &= -\frac{13}{12N} + \frac{5 \ln 2}{6N} - \lambda \left( \frac{1}{6N} - \frac{\ln 2}{6N} \right), \\
\left[ \Delta r_{\text{MS} \rightarrow \text{RI}}^{\text{SLL}} \right]_{31} &= 4N - \frac{12}{N} + \frac{40 \ln 2}{N} + \lambda \left( 6N - \frac{8}{N} + \frac{8 \ln 2}{N} \right), \\
\left[ \Delta r_{\text{MS} \rightarrow \text{RI}}^{\text{SLL}} \right]_{32} &= 8 - 40 \ln 2 + \lambda (2 - 8 \ln 2), \\
\left[ \Delta r_{\text{MS} \rightarrow \text{RI}}^{\text{SLL}} \right]_{33} &= -\frac{5N}{2} - \frac{5}{3N} + \frac{26 \ln 2}{3N} - \lambda \left( N + \frac{5}{6N} - \frac{10 \ln 2}{3N} \right), \\
\left[ \Delta r_{\text{MS} \rightarrow \text{RI}}^{\text{SLL}} \right]_{34} &= \frac{25}{6} - \frac{26 \ln 2}{3} + \lambda \left( \frac{11}{6} - \frac{10 \ln 2}{3} \right), \\
\left[ \Delta r_{\text{MS} \rightarrow \text{RI}}^{\text{SLL}} \right]_{41} &= 12 - 40 \ln 2 + \lambda (8 - 8 \ln 2),
\end{aligned}$$

$$\begin{aligned}
\left[\Delta r_{\overline{\text{MS}}\rightarrow\text{RI}}^{\text{SLL}}\right]_{42} &= -\frac{12}{N} + \frac{40\ln 2}{N} - \lambda\left(\frac{8}{N} - \frac{8\ln 2}{N}\right), \\
\left[\Delta r_{\overline{\text{MS}}\rightarrow\text{RI}}^{\text{SLL}}\right]_{43} &= \frac{5}{3} - \frac{26\ln 2}{3} + \lambda\left(\frac{1}{3} - \frac{10\ln 2}{3}\right), \\
\left[\Delta r_{\overline{\text{MS}}\rightarrow\text{RI}}^{\text{SLL}}\right]_{44} &= -\frac{5}{3N} + \frac{26\ln 2}{3N} + \lambda\left(\frac{N}{2} - \frac{5}{6N} + \frac{10\ln 2}{3N}\right).
\end{aligned}$$

In section 7, the above results will be used in performing the comparison with ref. [4].

## 6 Recovering the ADM of $\Delta F = 2$ operators from $\Delta F = 1$ results

Let us now use our  $\Delta F = 1$  anomalous dimensions from section 3 to find again the ADM of  $\Delta F = 2$  operators. This will serve as a cross-check of our findings and as a preparation for the comparison with ref. [4] in section 7.

Starting from eq. (3.1), we shall pass to another operator basis where the operators are either symmetric or antisymmetric under  $d \leftrightarrow c$  interchange. Next, the flavours of both quarks and both antiquarks will be set equal. For definiteness, we shall do it first in the SLL sector. The superscript ‘‘SLL’’ will be understood for all the relevant quantities below, and we shall not write it explicitly.

In four spacetime dimensions, passing to the new operator basis would be equivalent to performing a simple linear transformation of the operators. In the framework of dimensional regularization, introducing additional evanescent operators becomes necessary. In the SLL sector, only two evanescent operators were needed in the  $\Delta F = 1$  calculation (see appendix B). Now, we need to introduce six additional evanescent operators in this sector. They are defined in appendix C.

We begin with a redefinition of the physical operators  $Q_i$  ( $i = 1, \dots, 4$ ) that amounts to adding to them appropriate linear combinations of the evanescent operators  $E_i$ :

$$Q_i \rightarrow Q_i + \sum_{k=1}^8 W_{ik} E_k \equiv [Q_i]_{\text{new}} \quad (6.1)$$

where

$$\hat{W} = \begin{pmatrix} 0 & 0 & -\frac{1}{2} & 0 & \frac{1}{8} & 0 & 0 & 0 \\ 0 & 0 & 0 & 0 & 0 & 0 & 0 & 0 \\ 0 & 0 & 6 & 0 & \frac{1}{2} & 0 & 0 & 0 \\ 0 & 0 & 0 & 0 & 0 & 0 & 0 & 0 \end{pmatrix}. \quad (6.2)$$

The “new” operators read

$$[Q_1]_{\text{new}} = -\frac{1}{2}[Q_1]_F + \frac{1}{8}[Q_3]_F, \quad [Q_2]_{\text{new}} = Q_2, \quad (6.3)$$

$$[Q_3]_{\text{new}} = 6[Q_1]_F + \frac{1}{2}[Q_3]_F, \quad [Q_4]_{\text{new}} = Q_4, \quad (6.4)$$

where

$$[Q_1]_F = (\bar{s}^\alpha P_L c^\alpha) (\bar{u}^\beta P_L d^\beta), \quad [Q_3]_F = (\bar{s}^\alpha \sigma_{\mu\nu} P_L c^\alpha) (\bar{u}^\beta \sigma^{\mu\nu} P_L d^\beta). \quad (6.5)$$

In 4 spacetime dimensions, the transformation (6.1) would be equivalent to performing the Fierz rearrangement of  $Q_1$  and  $Q_3$ , as  $E_k$  would not contribute. Since the Fierz identities cannot be analytically continued to  $D$  dimensions, the Fierz rearrangement *must* be understood in terms of the transformation (6.1), so long as the  $\overline{\text{MS}}$  scheme is used. The  $\overline{\text{MS}}$ -renormalized one-loop matrix elements of  $Q_1$  and  $Q_3$  are affected by this transformation. This means that the renormalization scheme is changed. We pass from one version of the NDR- $\overline{\text{MS}}$  scheme to another, even though the evanescent operators remain unchanged.

After the redefinition (6.1), we perform a simple linear transformation of the operators

$$[Q_i]_{\text{new}} \rightarrow \sum_{j=1}^4 R_{ij} [Q_j]_{\text{new}} \quad (6.6)$$

with

$$\hat{R} = \begin{pmatrix} -\frac{1}{4} & \frac{1}{2} & \frac{1}{16} & 0 \\ 3 & 0 & \frac{1}{4} & \frac{1}{2} \\ \frac{1}{4} & \frac{1}{2} & -\frac{1}{16} & 0 \\ -3 & 0 & -\frac{1}{4} & \frac{1}{2} \end{pmatrix}. \quad (6.7)$$

As one can easily check, our final operator basis is  $\{Q_1^+, Q_2^+, Q_1^-, Q_2^-\}$ , where

$$\begin{aligned} Q_1^\pm &= \frac{1}{2} \left[ (\bar{s}^\alpha P_L d^\alpha) (\bar{u}^\beta P_L c^\beta) \pm (\bar{s}^\alpha P_L c^\alpha) (\bar{u}^\beta P_L d^\beta) \right], \\ Q_2^\pm &= \frac{1}{2} \left[ (\bar{s}^\alpha \sigma_{\mu\nu} P_L d^\alpha) (\bar{u}^\beta \sigma^{\mu\nu} P_L c^\beta) \pm (\bar{s}^\alpha \sigma_{\mu\nu} P_L c^\alpha) (\bar{u}^\beta \sigma^{\mu\nu} P_L d^\beta) \right]. \end{aligned} \quad (6.8)$$

The ADM transforms as follows:

$$\hat{\gamma}^{(0)} \rightarrow \hat{R}\hat{\gamma}^{(0)}\hat{R}^{-1}, \quad (6.9)$$

$$\hat{\gamma}^{(1)} \rightarrow \hat{R} \left\{ \hat{\gamma}^{(1)} + [\Delta\hat{r}, \hat{\gamma}^{(0)}] + 2\beta_0\Delta\hat{r} \right\} \hat{R}^{-1}, \quad (6.10)$$

where  $\beta_0 = \frac{11}{3}N - \frac{2}{3}f$ . The matrix  $\Delta\hat{r}$  reflects in the usual manner [14] change of the renormalization scheme that follows from eq. (6.1). The explicit form of  $\Delta\hat{r}$  is [8]

$$\Delta\hat{r} = -\hat{W}\hat{c}, \quad (6.11)$$

provided  $\hat{W}\hat{e} = 0$ . The matrices  $\hat{c}$  and  $\hat{e}$  are found from one-loop matrix elements of evanescent operators, as in eq. (2.16). The product  $\hat{W}\hat{e}$  indeed vanishes in our case, and

$$\hat{c} = \begin{pmatrix} * & * & * & * \\ * & * & * & * \\ \frac{3}{4}N - \frac{5}{N} & \frac{17}{4} & \frac{1}{16}N - \frac{1}{4N} & \frac{3}{16} \\ * & * & * & * \\ 7N - \frac{28}{N} & 21 & -\frac{7}{4}N + \frac{5}{N} & -\frac{13}{4} \\ * & * & * & * \\ * & * & * & * \\ * & * & * & * \end{pmatrix}. \quad (6.12)$$

Here, stars denote non-vanishing elements of  $\hat{c}$  that are irrelevant for us, since they do not affect the matrix

$$\Delta\hat{r} = -\hat{W}\hat{c} = \begin{pmatrix} -\frac{1}{2}N + \frac{1}{N} & -\frac{1}{2} & \frac{1}{4}N - \frac{3}{4N} & \frac{1}{2} \\ 0 & 0 & 0 & 0 \\ -8N + \frac{44}{N} & -36 & \frac{1}{2}N - \frac{1}{N} & \frac{1}{2} \\ 0 & 0 & 0 & 0 \end{pmatrix}. \quad (6.13)$$

After the transformation (6.9, 6.10), the ADM in the basis  $\{Q_1^+, Q_2^+, Q_1^-, Q_2^-\}$  is found to have the form

$$\hat{\gamma}_{4 \times 4} = \begin{pmatrix} \hat{\gamma}_{2 \times 2}^+ & 0_{2 \times 2} \\ 0_{2 \times 2} & \hat{\gamma}_{2 \times 2}^- \end{pmatrix}, \quad (6.14)$$

where  $\hat{\gamma}^\pm = \hat{\gamma}^{(0)\pm} + \frac{\alpha_s}{4\pi}\hat{\gamma}^{(1)\pm} + \dots$ ,

$$\hat{\gamma}^{(0)\pm} = \begin{pmatrix} -6N \pm 6 + \frac{6}{N} & \pm\frac{1}{2} - \frac{1}{N} \\ \mp 24 - \frac{48}{N} & 2N \pm 6 - \frac{2}{N} \end{pmatrix}, \quad (6.15)$$

and

$$\begin{aligned}
\gamma_{11}^{(1)\pm} &= -\frac{203}{6}N^2 \pm \frac{107}{3}N + \frac{136}{3} \mp \frac{12}{N} - \frac{107}{2N^2} + \frac{10}{3}Nf \mp \frac{2}{3}f - \frac{10}{3N}f, \\
\gamma_{12}^{(1)\pm} &= \mp \frac{1}{36}N - \frac{31}{9} \pm \frac{9}{N} - \frac{4}{N^2} \mp \frac{1}{18}f + \frac{1}{9N}f, \\
\gamma_{21}^{(1)\pm} &= \mp \frac{364}{3}N - \frac{704}{3} \mp \frac{208}{N} - \frac{320}{N^2} \pm \frac{136}{3}f + \frac{176}{3N}f, \\
\gamma_{22}^{(1)\pm} &= \frac{343}{18}N^2 \pm 21N - \frac{188}{9} \pm \frac{44}{N} + \frac{21}{2N^2} - \frac{26}{9}Nf \mp 6f + \frac{2}{9N}f.
\end{aligned} \tag{6.16}$$

One can easily verify that the matrix  $\hat{\gamma}^+$  is equal to the one we have already found in eqs. (2.18) and (2.20). It must be so, because the operators  $Q_i^+$  from eq. (6.8) reduce to  $Q_i^{\text{SLL}}$  from eq. (2.1) when the flavour replacements  $c \rightarrow d$  and  $\bar{u} \rightarrow \bar{s}$  are made. Moreover, the evanescent operators listed in appendices B and C can be linearly combined to the ones that are either symmetric or antisymmetric under  $d \leftrightarrow c$  interchange. When the flavour replacements  $c \rightarrow d$  and  $\bar{u} \rightarrow \bar{s}$  are made, the antisymmetric operators vanish, while the symmetric ones become equal to those in appendix A. Thus, we have shown how to extract the  $\Delta F = 2$  results from the  $\Delta F = 1$  ones.

Let us now briefly describe the analogous transformations in the VLL and  $\text{LR} \equiv \text{VLR} \oplus \text{SLR}$  sectors. All the necessary evanescent operators are given in appendices B and C. The relevant matrices  $\hat{W}$  and  $\hat{R}$  are the following:

$$\begin{aligned}
\hat{W}^{\text{VLL}} &= \begin{pmatrix} 0 & 0 & 1 & 0 & 0 & 0 \\ 0 & 0 & 0 & 0 & 0 & 0 \end{pmatrix}, \\
\hat{R}^{\text{VLL}} &= \frac{1}{2} \begin{pmatrix} 1 & 1 \\ -1 & 1 \end{pmatrix}, \\
\hat{W}_{4 \times 12}^{\text{LR}} &\equiv \begin{pmatrix} \hat{W}_{2 \times 6}^{\text{VLR}} & 0_{2 \times 6} \\ 0_{2 \times 6} & \hat{W}_{2 \times 6}^{\text{SLR}} \end{pmatrix} = \begin{pmatrix} -2\hat{W}^{\text{VLL}} & 0_{2 \times 6} \\ 0_{2 \times 6} & -\frac{1}{2}\hat{W}^{\text{VLL}} \end{pmatrix}, \\
\hat{R}^{\text{LR}} &= \frac{1}{2} \begin{pmatrix} 0 & 1 & -2 & 0 \\ -\frac{1}{2} & 0 & 0 & 1 \\ 0 & 1 & 2 & 0 \\ \frac{1}{2} & 0 & 0 & 1 \end{pmatrix}.
\end{aligned} \tag{6.17}$$

Consequently, the final operator bases are  $\{Q_1^{\text{VLL}+}, Q_1^{\text{VLL}-}\}$  and  $\{Q_1^{\text{LR}+}, Q_2^{\text{LR}+}, Q_1^{\text{LR}-}, Q_2^{\text{LR}-}\}$ , where

$$Q_1^{\text{VLL}\pm} = \frac{1}{2} \left[ (\bar{s}^\alpha \gamma_\mu P_L d^\alpha) (\bar{u}^\beta \gamma^\mu P_L c^\beta) \pm (\bar{s}^\alpha \gamma_\mu P_L c^\alpha) (\bar{u}^\beta \gamma^\mu P_L d^\beta) \right],$$

$$\begin{aligned}
Q_1^{LR\pm} &= \frac{1}{2} \left[ (\bar{s}^\alpha \gamma_\mu P_L d^\alpha) (\bar{u}^\beta \gamma^\mu P_R c^\beta) \pm (\bar{s}^\alpha \gamma_\mu P_R c^\alpha) (\bar{u}^\beta \gamma^\mu P_L d^\beta) \right], \\
Q_2^{LR\pm} &= \frac{1}{2} \left[ (\bar{s}^\alpha P_L d^\alpha) (\bar{u}^\beta P_R c^\beta) \pm (\bar{s}^\alpha P_R c^\alpha) (\bar{u}^\beta P_L d^\beta) \right].
\end{aligned} \tag{6.18}$$

An important simplification in the present case is that the one-loop matrix elements of the evanescent operators  $E_3^{\text{VLL}}$ ,  $E_3^{\text{VLR}}$  and  $E_3^{\text{SLR}}$  from appendix C vanish in the limit  $D \rightarrow 4$ , after subtraction of the MS-counterterms proportional to evanescent operators only. This means that the third rows of  $\hat{c}^{\text{VLL}}$ ,  $\hat{c}^{\text{VLR}}$  and  $\hat{c}^{\text{SLR}}$  vanish (cf. eq. (2.16)). Consequently,  $\Delta \hat{r}^{\text{VLL}} = -\hat{W}^{\text{VLL}} \hat{c}^{\text{VLL}} = 0$  and  $\Delta \hat{r}^{\text{LR}} = -\hat{W}^{\text{LR}} \hat{c}^{\text{LR}} = 0$ . This is why the two-loop  $\Delta F = 1$  matrices of the VLL, VLR and SLR sectors exhibited Fierz symmetry in eq. (3.10). The transformations of the two-loop ADMs in the VLL and LR sectors thus look as if we worked in 4 dimensions, i.e. they reduce to simple multiplications by the corresponding  $\hat{R}$ -matrices and their inversions. The final results are

$$\hat{\gamma}_{2 \times 2}^{\text{VLL}} = \begin{pmatrix} \hat{\gamma}^{\text{VLL}+} & 0 \\ 0 & \hat{\gamma}^{\text{VLL}-} \end{pmatrix}, \quad \hat{\gamma}_{4 \times 4}^{\text{LR}} = \begin{pmatrix} \hat{\gamma}_{2 \times 2}^{\text{LR}+} & \mathbf{0}_{2 \times 2} \\ \mathbf{0}_{2 \times 2} & \hat{\gamma}_{2 \times 2}^{\text{LR}-} \end{pmatrix}, \tag{6.19}$$

where

$$\begin{aligned}
\gamma^{(0)\text{VLL}\pm} &= \pm 6 - \frac{6}{N}, \\
\gamma^{(1)\text{VLL}\pm} &= \mp \frac{19}{6} N - \frac{22}{3} \pm \frac{39}{N} - \frac{57}{2N^2} \pm \frac{2}{3} f - \frac{2}{3N} f, \\
\hat{\gamma}^{(0)\text{LR}\pm} &= \begin{pmatrix} \frac{6}{N} & \pm 12 \\ 0 & -6N + \frac{6}{N} \end{pmatrix}, \\
\hat{\gamma}^{(1)\text{LR}\pm} &= \begin{pmatrix} \frac{137}{6} + \frac{15}{2N^2} - \frac{22}{3N} f & \pm \frac{200}{3} N \mp \frac{6}{N} \mp \frac{44}{3} f \\ \pm \frac{71}{4} N \pm \frac{9}{N} \mp 2f & -\frac{203}{6} N^2 + \frac{479}{6} + \frac{15}{2N^2} + \frac{10}{3} N f - \frac{22}{3N} f \end{pmatrix}.
\end{aligned} \tag{6.20}$$

One can see that  $\gamma^{\text{VLL}+}$  and  $\hat{\gamma}^{\text{LR}+}$  are identical to our  $\Delta F = 2$  results in eqs. (2.21), (2.23) and (2.24).



## 7 Comparison with previous ADM calculations

In the present section, we compare our findings from sections 2, 3 and 4 with the previously published results for anomalous-dimension matrices.

### 7.1 One-loop results

As far as the one-loop QCD ADMs of four-quark operators are concerned, the historical order of their evaluation was as follows:

- Current–current contributions to the one-loop ADM of  $\Delta F = 1$  operators belonging to the VLL and VLR sectors were originally calculated in refs. [15, 16]. These results were also immediately applicable to the SLR sector, because the Fierz rearrangement has a trivial effect at one loop. For the same reason, one-loop anomalous dimensions of the  $\Delta F = 2$  operators belonging to the VLL and LR sectors could have been immediately read off from these articles. Thus, after 1974, the only unpublished one-loop current–current anomalous dimensions were those of the SLL sector, both in the  $\Delta F = 1$  and  $\Delta F = 2$  cases.
- One-loop penguin contributions to the ADM of the Standard Model operators were originally evaluated in refs. [17]–[19]. As we have shown in section 4, penguin contributions to the ADM of other (beyond–SM) flavour-changing dimension-six operators can be easily extracted from the SM calculations, both at one and at two loops.
- To our knowledge, the first published results for  $\gamma^{(0)\text{SLL}}$  occur in refs. [20] and [4], for the  $\Delta F = 2$  and  $\Delta F = 1$  cases, respectively.

The one-loop ADMs given in the present article agree with all the papers quoted above. However, in order to perform comparisons, one often needs to make simple linear transformations, because different operator bases are used by different authors. For instance, the results for  $\hat{\gamma}^{(0)\text{SLL}}$  in ref. [20] are given in the basis  $\{Q_1^{\text{SLL}}, \tilde{Q}_1^{\text{SLL}}\}$ . In order to compare them with our eq. (2.18), one should use the relation (2.6). Similarly, eqs. (6.7) and (6.9) need to be used for comparing our  $\hat{\gamma}^{(0)\text{SLL}}$  in eq. (3.8) with the corresponding results in ref. [4].

## 7.2 Two-loop results

The history of previous two-loop computations is as follows:

- The current–current anomalous dimensions of the  $\Delta F = 1$  operators belonging to the VLL sector were originally calculated in ref. [21] (in the DRED– $\overline{\text{MS}}$  scheme), and confirmed in ref. [5] (where the NDR– $\overline{\text{MS}}$  and HV– $\overline{\text{MS}}$  results were also given).
- The remaining elements of the two-loop QCD ADM for  $\Delta F = 1$  operators relevant in the SM were calculated in refs. [6, 7]. New results in these papers were the current–current contributions in the VLR sector, as well as all the penguin contributions. The SLR sector results in the  $\Delta F = 1$  case, as well as the  $\Delta F = 2$  results for the VLL and LR sectors could be easily derived from them with the help of Fierz identities, because the NDR– $\overline{\text{MS}}$ -renormalized one-loop matrix elements remain invariant under Fierz transformations, except for the current–current ones in the SLL sector, and the penguin ones in the VLL sector. Therefore, in the early 1990’s, the only unknown two-loop anomalous dimensions were those of the SLL sector.
- The first calculation of the two-loop ADM in the SLL sector was performed by Ciuchini et al. [4], in both the  $\Delta F = 1$  and  $\Delta F = 2$  cases. The ADM was calculated there in the so-called “FRI” renormalization scheme. The transformation rules were given to the LRI scheme (Landau-gauge RI-scheme) and to the NDR– $\overline{\text{MS}}$  scheme. Current–current anomalous dimensions for the remaining sectors were recalculated as well.
- Penguin contributions to the ADM of non-SM operators are considered for the first time in the present article.

All the two-loop results presented here agree with the previous calculations mentioned above, except for the NDR– $\overline{\text{MS}}$  ones for the SLL sector found in ref. [4]. Below, we explain the reason for this disagreement.

### 7.3 Comparison with ref. [4]

In ref. [4], the two-loop ADM for  $\Delta F = 1$  operators of the SLL sector was given in the basis defined in eq. (13) of that paper, which is equivalent to our eq. (6.8). It was presented in the so-called ‘‘FRI’’ renormalization scheme, and the transformation rules to the NDR- $\overline{\text{MS}}$  scheme were appended. Applying these transformation rules to their ‘‘FRI’’-scheme ADM, one obtains results that differ from our eq. (6.16). In particular, a mixing between  $Q_i^-$  and  $Q_i^+$  occurs, which is absent in our result (6.16). We could obtain their result if we ignored the transformation (6.1) and, consequently, used  $\Delta\hat{r} = 0$  in our eq. (6.10). However, the final results would then correspond to the basis

$$\begin{aligned} Q_1^{\pm} &= \frac{1}{2} \left[ (\bar{s}^\alpha P_L d^\alpha)(\bar{u}^\beta P_L c^\beta) \mp \frac{1}{2}(\bar{s}^\alpha P_L d^\beta)(\bar{u}^\beta P_L c^\alpha) \pm \frac{1}{8}(\bar{s}^\alpha \sigma_{\mu\nu} P_L d^\beta)(\bar{u}^\beta \sigma^{\mu\nu} P_L c^\alpha) \right], \\ Q_2^{\pm} &= \frac{1}{2} \left[ (\bar{s}^\alpha \sigma_{\mu\nu} P_L d^\alpha)(\bar{u}^\beta \sigma^{\mu\nu} P_L c^\beta) \pm 6(\bar{s}^\alpha P_L d^\beta)(\bar{u}^\beta P_L c^\alpha) \pm \frac{1}{2}(\bar{s}^\alpha \sigma_{\mu\nu} P_L d^\beta)(\bar{u}^\beta \sigma^{\mu\nu} P_L c^\alpha) \right], \end{aligned} \quad (7.1)$$

rather than the one in eq. (6.8). In 4 spacetime dimensions, the operators (6.8) and (7.1) are identical, thanks to the Fierz identities (2.5). However, in  $D$  dimensions they are not. Consequently, their NDR- $\overline{\text{MS}}$ -renormalized matrix elements differ at one loop, and it is not surprising that the two-loop ADM depends on which of the two bases is used.

We informed the authors of ref. [4] about our findings prior to publication of the present article. They responded that although their NDR- $\overline{\text{MS}}$  results had been claimed to correspond to the basis (6.8), the NDR- $\overline{\text{MS}}$  renormalization conditions had been actually imposed in the basis (7.1). However, they had forgotten to mention this in their article. Unfortunately, such a mistake in the presentation has the same effect on the final result as a mistake in the calculation that amounts to missing  $\Delta\hat{r} \neq 0$  in eq. (6.10).

As far as the two-loop ADM for  $\Delta F = 2$  operators of the SLL sector is concerned, the situation is as follows. If we made the flavour replacements  $c \rightarrow d$  and  $\bar{u} \rightarrow \bar{s}$  in the basis (7.1), but did not change anything in the ADM, we could interpret this ADM as the one for  $\Delta F = 2$  operators, as the authors of ref. [4] did. However, it would correspond to quite non-standard conventions for the treatment of the evanescent operators obtained from  $Q_1^-$  and  $Q_2^-$  after

the flavour replacements. One would need to assume that the finite one-loop matrix elements of these evanescent operators are not renormalized away, contrary to the usual procedure for any evanescent operator [5, 8, 10, 11]. Such non-standard conventions make the RGE evolution more complicated, because one has to deal with a  $4 \times 4$  instead of a  $2 \times 2$  ADM in the NDR- $\overline{\text{MS}}$  RGE for the SLL sector, in the  $\Delta F = 2$  case. The calculation of the one-loop matrix elements becomes more involved, as well.

In the  $\Delta F = 2$  case, no calculation is necessary to convince oneself that the results of ref. [4] cannot correspond to the NDR- $\overline{\text{MS}}$  renormalization conditions imposed in the basis (6.8) (their eq. (13)). Once the  $c \rightarrow d$  and  $\bar{u} \rightarrow \bar{s}$  replacements have been made, the operators  $Q_i^-$  in eq. (6.8) vanish identically in  $D$  dimensions. Therefore, they cannot mix into the  $Q_i^+$  operators, independently of what the treatment of evanescent operators is. On the other hand, mixing of  $Q_i^-$  into  $Q_i^+$  was claimed to be found in the NDR- $\overline{\text{MS}}$  scheme in ref. [4]. Therefore, an inconsistency is clearly seen.

In the remainder of this section, we shall verify that our NDR- $\overline{\text{MS}}$  results are compatible with the LRI ones of ref. [4]. By differentiating eq. (5.14) with respect to  $\mu$ , one obtains

$$\begin{aligned} \hat{\gamma}_{\text{RI}}^T(\mu) \vec{C}^{\text{RI}}(\mu) &= \left[ \frac{\beta_0 \alpha_s^2(\mu)}{8\pi^2} \Delta \hat{r}_{\overline{\text{MS}} \rightarrow \text{RI}}^T(\mu) + \frac{\beta_\lambda^0 \alpha_s(\mu)}{8\pi^2} \lambda(\mu) \left( \frac{\partial}{\partial \lambda} \Delta \hat{r}_{\overline{\text{MS}} \rightarrow \text{RI}}^T(\mu) \right) \right. \\ &\quad \left. + \left( 1 - \frac{\alpha_s(\mu)}{4\pi} \Delta \hat{r}_{\overline{\text{MS}} \rightarrow \text{RI}}^T(\mu) \right) \hat{\gamma}_{\overline{\text{MS}}}^T(\mu) \right] \vec{C}^{\overline{\text{MS}}}(\mu) + \mathcal{O}(\alpha_s^3), \end{aligned} \quad (7.2)$$

where we have used the RGE (2.11),

$$\mu \frac{d}{d\mu} \alpha_s(\mu) = -\frac{\beta_0 \alpha_s(\mu)^2}{2\pi} + \mathcal{O}(\alpha_s^3) \quad \text{and} \quad \mu \frac{d}{d\mu} \lambda(\mu) = -\frac{\beta_\lambda^0 \alpha_s(\mu)}{2\pi} \lambda(\mu) + \mathcal{O}(\alpha_s^2). \quad (7.3)$$

We have also used the fact that the dependence of  $\Delta \hat{r}_{\overline{\text{MS}} \rightarrow \text{RI}}$  on  $\mu$  originates solely from its dependence on the gauge-fixing parameter  $\lambda(\mu)$ .

Next, we use eq. (5.14) again to express  $\vec{C}^{\overline{\text{MS}}}(\mu)$  by  $\vec{C}^{\text{RI}}(\mu)$  in eq. (7.2). Then, the first two terms of the perturbative expansion (2.12) of  $\hat{\gamma}_{\text{RI}}$  can be easily read off

$$\hat{\gamma}_{\text{RI}}^{(0)} = \hat{\gamma}_{\overline{\text{MS}}}^{(0)}, \quad (7.4)$$

$$\hat{\gamma}_{\text{RI}}^{(1)} = \hat{\gamma}_{\overline{\text{MS}}}^{(1)} + \left[ \Delta \hat{r}_{\overline{\text{MS}} \rightarrow \text{RI}}, \hat{\gamma}_{\overline{\text{MS}}}^{(0)} \right] + 2 \left( \beta_0 + \beta_\lambda^0 \lambda \frac{\partial}{\partial \lambda} \right) \Delta \hat{r}_{\overline{\text{MS}} \rightarrow \text{RI}}. \quad (7.5)$$

Armed with our explicit expressions for  $\Delta\hat{r}_{\overline{\text{MS}}\rightarrow\text{RI}}$  given in section 5 and with the values of

$$\beta_0 = \frac{11}{3}N - \frac{2}{3}f \quad \text{and} \quad \beta_\lambda^0 = \left(\frac{\lambda}{2} - \frac{13}{6}\right)N + \frac{2}{3}f, \quad (7.6)$$

we can easily calculate the RI-scheme ADM from our  $\overline{\text{MS}}$  results, for arbitrary  $\lambda$ . Setting then  $\lambda \rightarrow 0$ , we recover all the LRI-scheme anomalous dimensions given in ref. [4].

As far as the ‘‘FRI’’-scheme ADMs of ref. [4] are concerned, we can confirm them as well. However, it should be emphasized that the ‘‘FRI’’ scheme is not equivalent to the RI scheme considered in section 5 for any choice of  $\lambda$ . The ‘‘FRI’’ scheme cannot be defined beyond perturbation theory, because different external momenta are chosen in different diagrams when the renormalization conditions are specified. Therefore, in our opinion, the main advantage of the RI scheme is lost.

## 8 Conclusions

In the present paper, we have calculated the two-loop QCD anomalous dimensions matrix (ADM)  $(\hat{\gamma}^{(1)})_{\text{NDR}}$  in the  $\text{NDR-}\overline{\text{MS}}$  scheme for all the four-fermion dimension-six flavour-changing operators that are relevant to both the Standard Model and its extensions.

The  $\Delta F = 2$  two-loop results can be found in eqs. (2.20), (2.21) and (2.24). While the matrices in eqs. (2.21) and (2.24) could be extracted from the already published results, the two-loop  $\text{NDR-}\overline{\text{MS}}$  ADM (2.20) for the SLL operators defined in eq. (2.1) is correctly calculated for the first time here.

The  $\Delta F = 1$  two-loop results for operators containing four different quark flavours can be found in eqs. (3.3), (3.5), (3.7) and (3.9). While the matrices in eqs. (3.3), (3.5) and (3.7) could be extracted from the already published results, the two-loop  $\text{NDR-}\overline{\text{MS}}$  ADM (3.9) for the SLL operators defined in eq. (3.1) is correctly calculated for the first time here.

Penguin contributions to the ADM of non-SM operators have been considered for the first time here. These contributions can be easily extracted from the existing SM calculations. We have identified the relevant non-SM operators in the  $\Delta S = 1$  case, and presented the corresponding ADM explicitly in eqs. (4.8) and (4.9).

We have demonstrated that the main findings of our paper, given in eqs. (2.20) and (3.9), are compatible with each other, i.e. we have shown how to properly transform the ADMs from the  $\Delta F = 1$  to the  $\Delta F = 2$  case. In this context, we have pointed out that in the process of this transformation it is necessary to introduce additional evanescent operators that vanish in four spacetime dimensions because of the Fierz identities.

We have also given the rules that allow transforming our NDR- $\overline{\text{MS}}$  ADMs to the corresponding results in the RI scheme, for arbitrary gauge-fixing parameter  $\lambda$ . They can be found in the end of section 5.

The  $\Delta F = 1$  two-loop ADMs for all the operators defined in eq. (3.1) were previously presented in ref. [4], in the  $Q_i^\pm$  basis. In the case of VLL, VLR and SLR operators, there is full agreement between their and our results. The case of SLL operators is more subtle. We can confirm their LRI-scheme results (RI scheme with  $\lambda = 0$ ). However, their NDR- $\overline{\text{MS}}$  ADM is compatible with ours *only* after correcting their eq. (13), i.e. after changing the definitions of their SLL operators to the ones given in eq. (7.1).

After such a correction in eq. (13) of ref. [4], also their  $\Delta F = 2$  NDR- $\overline{\text{MS}}$  results are compatible with ours, provided they are understood in terms of quite non-standard conventions for the treatment of evanescent operators. In their conventions, the two-loop  $\Delta F = 2$  NDR- $\overline{\text{MS}}$  ADM is a  $4 \times 4$  rather than  $2 \times 2$  matrix, which makes the RGE evolution and calculating low-energy matrix elements unnecessarily complicated. Consequently, the results presented here should be more useful for phenomenological applications.

## Acknowledgements

We thank the authors of ref. [4] for extensive discussions concerning their paper. Furthermore, we would like to thank Christoph Bobeth and Gerhard Buchalla for carefully reading the manuscript. A.B. and J.U. acknowledge support from the German Bundesministerium für Bildung und Forschung under the contract O5HT9WOA0. M.M. has been supported in part by the Polish Committee for Scientific Research under grant 2 P03B 014 14, 1998-2000.

## Appendix A

Here, we specify the evanescent operators that are necessary as counterterms for one-loop diagrams with insertions of the  $\Delta F = 2$  operators (2.1).

$$\begin{aligned}
E_1^{\text{VLL}} &= (\bar{s}^\alpha \gamma_\mu P_L d^\beta)(\bar{s}^\beta \gamma^\mu P_L d^\alpha) - Q_1^{\text{VLL}}, \\
E_2^{\text{VLL}} &= (\bar{s}^\alpha \gamma_\mu \gamma_\nu \gamma_\rho P_L d^\alpha)(\bar{s}^\beta \gamma^\mu \gamma^\nu \gamma^\rho P_L d^\beta) + (-16 + 4\epsilon)Q_1^{\text{VLL}}, \\
E_3^{\text{VLL}} &= (\bar{s}^\alpha \gamma_\mu \gamma_\nu \gamma_\rho P_L d^\beta)(\bar{s}^\beta \gamma^\mu \gamma^\nu \gamma^\rho P_L d^\alpha) + (-16 + 4\epsilon)Q_1^{\text{VLL}}, \\
E_1^{\text{LR}} &= (\bar{s}^\alpha P_L d^\beta)(\bar{s}^\beta P_R d^\alpha) + \frac{1}{2}Q_1^{\text{LR}}, \\
E_2^{\text{LR}} &= (\bar{s}^\alpha \gamma_\mu P_L d^\beta)(\bar{s}^\beta \gamma^\mu P_R d^\alpha) + 2Q_2^{\text{LR}}, \\
E_3^{\text{LR}} &= (\bar{s}^\alpha \gamma_\mu \gamma_\nu \gamma_\rho P_L d^\alpha)(\bar{s}^\beta \gamma^\mu \gamma^\nu \gamma^\rho P_R d^\beta) + (-4 - 4\epsilon)Q_1^{\text{LR}}, \\
E_4^{\text{LR}} &= (\bar{s}^\alpha \gamma_\mu \gamma_\nu \gamma_\rho P_L d^\beta)(\bar{s}^\beta \gamma^\mu \gamma^\nu \gamma^\rho P_R d^\alpha) + (8 + 8\epsilon)Q_2^{\text{LR}}, \\
E_5^{\text{LR}} &= (\bar{s}^\alpha \sigma_{\mu\nu} P_L d^\alpha)(\bar{s}^\beta \sigma^{\mu\nu} P_R d^\beta) - 6\epsilon Q_2^{\text{LR}}, \\
E_6^{\text{LR}} &= (\bar{s}^\alpha \sigma_{\mu\nu} P_L d^\beta)(\bar{s}^\beta \sigma^{\mu\nu} P_R d^\alpha) + 3\epsilon Q_1^{\text{LR}}, \\
E_1^{\text{SLL}} &= (\bar{s}^\alpha P_L d^\beta)(\bar{s}^\beta P_L d^\alpha) + \frac{1}{2}Q_1^{\text{SLL}} - \frac{1}{8}Q_2^{\text{SLL}}, \\
E_2^{\text{SLL}} &= (\bar{s}^\alpha \sigma_{\mu\nu} P_L d^\beta)(\bar{s}^\beta \sigma^{\mu\nu} P_L d^\alpha) - 6Q_1^{\text{SLL}} - \frac{1}{2}Q_2^{\text{SLL}}, \\
E_3^{\text{SLL}} &= (\bar{s}^\alpha \gamma_\mu \gamma_\nu \gamma_\rho \gamma_\sigma P_L d^\alpha)(\bar{s}^\beta \gamma^\mu \gamma^\nu \gamma^\rho \gamma^\sigma P_L d^\beta) + (-64 + 96\epsilon)Q_1^{\text{SLL}} + (-16 + 8\epsilon)Q_2^{\text{SLL}}, \\
E_4^{\text{SLL}} &= (\bar{s}^\alpha \gamma_\mu \gamma_\nu \gamma_\rho \gamma_\sigma P_L d^\beta)(\bar{s}^\beta \gamma^\mu \gamma^\nu \gamma^\rho \gamma^\sigma P_L d^\alpha) - 64Q_1^{\text{SLL}} + (-16 + 16\epsilon)Q_2^{\text{SLL}}.
\end{aligned}$$

The evanescent operators for the VRR and SRR sectors, i.e.  $E_k^{\text{VRR}}$  and  $E_k^{\text{SRR}}$  are obtained by replacing  $L$  by  $R$  in the definitions of  $E_k^{\text{VLL}}$  and  $E_k^{\text{SLL}}$ .

The operators  $E_1^{\text{VLL}}$ ,  $E_1^{\text{LR}}$ ,  $E_2^{\text{LR}}$ ,  $E_1^{\text{SLL}}$  and  $E_2^{\text{SLL}}$  vanish in four spacetime dimensions because of the Fierz identities (3.11), (3.12) and (2.5). The operators  $E_2^{\text{VLL}}$ ,  $E_3^{\text{VLL}}$ ,  $E_3^{\text{LR}}$ ,  $E_4^{\text{LR}}$ ,  $E_3^{\text{SLL}}$  and  $E_4^{\text{SLL}}$  vanish by the four-dimensional identity (2.2). Finally,  $E_5^{\text{LR}}$  and  $E_6^{\text{LR}}$  vanish in four dimensions, because they become full contractions of self-dual and self-antidual antisymmetric tensors.

The evanescent operators listed here would look somewhat simpler if we removed from them all the terms proportional to  $\epsilon$ . It would be equivalent to changing one version of the  $\overline{\text{MS}}$  scheme to another. Keeping the terms proportional to  $\epsilon$  in the above equations makes our NDR- $\overline{\text{MS}}$

scheme equivalent to the one where the so-called ‘‘Greek projections’’ are used (see appendix D).

## Appendix B

Here, we specify the evanescent operators that are necessary as counterterms for one-loop diagrams with insertions of the  $\Delta F = 1$  operators (3.1).

$$\begin{aligned}
E_1^{\text{VLL}} &= (\bar{s}^\alpha \gamma_\mu \gamma_\nu \gamma_\rho P_L d^\beta) (\bar{u}^\beta \gamma^\mu \gamma^\nu \gamma^\rho P_L c^\alpha) + (-16 + 4\epsilon) Q_1^{\text{VLL}}, \\
E_2^{\text{VLL}} &= (\bar{s}^\alpha \gamma_\mu \gamma_\nu \gamma_\rho P_L d^\alpha) (\bar{u}^\beta \gamma^\mu \gamma^\nu \gamma^\rho P_L c^\beta) + (-16 + 4\epsilon) Q_2^{\text{VLL}}, \\
E_1^{\text{VLR}} &= (\bar{s}^\alpha \gamma_\mu \gamma_\nu \gamma_\rho P_L d^\beta) (\bar{u}^\beta \gamma^\mu \gamma^\nu \gamma^\rho P_R c^\alpha) + (-4 - 4\epsilon) Q_1^{\text{VLR}}, \\
E_2^{\text{VLR}} &= (\bar{s}^\alpha \gamma_\mu \gamma_\nu \gamma_\rho P_L d^\alpha) (\bar{u}^\beta \gamma^\mu \gamma^\nu \gamma^\rho P_R c^\beta) + (-4 - 4\epsilon) Q_2^{\text{VLR}}, \\
E_1^{\text{SLR}} &= (\bar{s}^\alpha \sigma_{\mu\nu} P_L d^\beta) (\bar{u}^\beta \sigma^{\mu\nu} P_R c^\alpha) - 6\epsilon Q_1^{\text{SLR}}, \\
E_2^{\text{SLR}} &= (\bar{s}^\alpha \sigma_{\mu\nu} P_L d^\alpha) (\bar{u}^\beta \sigma^{\mu\nu} P_R c^\beta) - 6\epsilon Q_2^{\text{SLR}}, \\
E_1^{\text{SLL}} &= (\bar{s}^\alpha \gamma_\mu \gamma_\nu \gamma_\rho \gamma_\sigma P_L d^\beta) (\bar{u}^\beta \gamma^\mu \gamma^\nu \gamma^\rho \gamma^\sigma P_L c^\alpha) + (-64 + 96\epsilon) Q_1^{\text{SLL}} + (-16 + 8\epsilon) Q_3^{\text{SLL}}, \\
E_2^{\text{SLL}} &= (\bar{s}^\alpha \gamma_\mu \gamma_\nu \gamma_\rho \gamma_\sigma P_L d^\alpha) (\bar{u}^\beta \gamma^\mu \gamma^\nu \gamma^\rho \gamma^\sigma P_L c^\beta) + (-64 + 96\epsilon) Q_2^{\text{SLL}} + (-16 + 8\epsilon) Q_4^{\text{SLL}}.
\end{aligned}$$

The remaining evanescent operators (for the VRR, VRL, SRL and SRR sectors) are obtained by interchanging  $L$  and  $R$  above.

## Appendix C

This appendix contains definitions of the ‘‘additional’’ evanescent operators that are *not* necessary as one-loop counterterms in the  $\Delta F = 1$  effective Lagrangian in section 3. However, they have to be included before performing transformation to the ‘‘plus–minus’’ basis in section 6.

$$\begin{aligned}
E_3^{\text{VLL}} &= (\bar{s}^\alpha \gamma_\mu P_L c^\alpha) (\bar{u}^\beta \gamma^\mu P_L d^\beta) - Q_1^{\text{VLL}}, \\
E_4^{\text{VLL}} &= (\bar{s}^\alpha \gamma_\mu P_L c^\beta) (\bar{u}^\beta \gamma^\mu P_L d^\alpha) - Q_2^{\text{VLL}}, \\
E_5^{\text{VLL}} &= (\bar{s}^\alpha \gamma_\mu \gamma_\nu \gamma_\rho P_L c^\alpha) (\bar{u}^\beta \gamma^\mu \gamma^\nu \gamma^\rho P_L d^\beta) + (-16 + 4\epsilon) Q_1^{\text{VLL}}, \\
E_6^{\text{VLL}} &= (\bar{s}^\alpha \gamma_\mu \gamma_\nu \gamma_\rho P_L c^\beta) (\bar{u}^\beta \gamma^\mu \gamma^\nu \gamma^\rho P_L d^\alpha) + (-16 + 4\epsilon) Q_2^{\text{VLL}},
\end{aligned}$$



$$\begin{aligned}
E_3^{\text{VLR}} &= (\bar{s}^\alpha P_R c^\alpha)(\bar{u}^\beta P_L d^\beta) + \frac{1}{2}Q_1^{\text{VLR}}, \\
E_4^{\text{VLR}} &= (\bar{s}^\alpha P_R c^\beta)(\bar{u}^\beta P_L d^\alpha) + \frac{1}{2}Q_2^{\text{VLR}}, \\
E_5^{\text{VLR}} &= (\bar{s}^\alpha \sigma_{\mu\nu} P_R c^\alpha)(\bar{u}^\beta \sigma^{\mu\nu} P_L d^\beta) + 3\epsilon Q_1^{\text{VLR}}, \\
E_6^{\text{VLR}} &= (\bar{s}^\alpha \sigma_{\mu\nu} P_R c^\beta)(\bar{u}^\beta \sigma^{\mu\nu} P_L d^\alpha) + 3\epsilon Q_2^{\text{VLR}}, \\
\\
E_3^{\text{SLR}} &= (\bar{s}^\alpha \gamma_\mu P_R c^\alpha)(\bar{u}^\beta \gamma^\mu P_L d^\beta) + 2Q_1^{\text{SLR}}, \\
E_4^{\text{SLR}} &= (\bar{s}^\alpha \gamma_\mu P_R c^\beta)(\bar{u}^\beta \gamma^\mu P_L d^\alpha) + 2Q_2^{\text{SLR}}, \\
E_5^{\text{SLR}} &= (\bar{s}^\alpha \gamma_\mu \gamma_\nu \gamma_\rho P_R c^\alpha)(\bar{u}^\beta \gamma^\mu \gamma^\nu \gamma^\rho P_L d^\beta) + (8 + 8\epsilon)Q_1^{\text{SLR}}, \\
E_6^{\text{SLR}} &= (\bar{s}^\alpha \gamma_\mu \gamma_\nu \gamma_\rho P_R c^\beta)(\bar{u}^\beta \gamma^\mu \gamma^\nu \gamma^\rho P_L d^\alpha) + (8 + 8\epsilon)Q_2^{\text{SLR}}, \\
\\
E_3^{\text{SLL}} &= (\bar{s}^\alpha P_L c^\alpha)(\bar{u}^\beta P_L d^\beta) + \frac{1}{2}Q_1^{\text{SLL}} - \frac{1}{8}Q_3^{\text{SLL}}, \\
E_4^{\text{SLL}} &= (\bar{s}^\alpha P_L c^\beta)(\bar{u}^\beta P_L d^\alpha) + \frac{1}{2}Q_2^{\text{SLL}} - \frac{1}{8}Q_4^{\text{SLL}}, \\
E_5^{\text{SLL}} &= (\bar{s}^\alpha \sigma_{\mu\nu} P_L c^\alpha)(\bar{u}^\beta \sigma^{\mu\nu} P_L d^\beta) - 6Q_1^{\text{SLL}} - \frac{1}{2}Q_3^{\text{SLL}}, \\
E_6^{\text{SLL}} &= (\bar{s}^\alpha \sigma_{\mu\nu} P_L c^\beta)(\bar{u}^\beta \sigma^{\mu\nu} P_L d^\alpha) - 6Q_2^{\text{SLL}} - \frac{1}{2}Q_4^{\text{SLL}}, \\
E_7^{\text{SLL}} &= (\bar{s}^\alpha \gamma_\mu \gamma_\nu \gamma_\rho \gamma_\sigma P_L c^\alpha)(\bar{u}^\beta \gamma^\mu \gamma^\nu \gamma^\rho \gamma^\sigma P_L d^\beta) - 64Q_1^{\text{SLL}} + (-16 + 16\epsilon)Q_3^{\text{SLL}}, \\
E_8^{\text{SLL}} &= (\bar{s}^\alpha \gamma_\mu \gamma_\nu \gamma_\rho \gamma_\sigma P_L c^\beta)(\bar{u}^\beta \gamma^\mu \gamma^\nu \gamma^\rho \gamma^\sigma P_L d^\alpha) - 64Q_2^{\text{SLL}} + (-16 + 16\epsilon)Q_4^{\text{SLL}}.
\end{aligned}$$

The remaining evanescent operators (for the VRR, VRL, SRL and SRR sectors) are obtained by interchanging  $L$  and  $R$  above.

## Appendix D

In the present appendix, the notion of ‘‘Greek projections’’ [2, 5, 22] is recalled and generalized to the case of SLL-sector operators. Let us denote the Dirac structure of the operator in eq. (1.1) by  $\Gamma_A \otimes \Gamma_B$ . The insertion of this operator in one- and two-loop diagrams results in new Dirac structures like

$$\Gamma_n \Gamma_A \otimes \Gamma^n \Gamma_B, \tag{D.1}$$

where  $\Gamma_n = \gamma_{\mu_1} \gamma_{\mu_2} \dots \gamma_{\mu_n}$ . Several examples of such structures occur in appendices A–C. It has

been suggested in ref. [22] to project them onto physical operators as follows. One defines the projection  $G$  so that the following equality is satisfied

$$G[\Gamma_n \Gamma_A \otimes \Gamma^n \Gamma_B] = \xi G[\Gamma^A \otimes \Gamma^B]. \quad (\text{D.2})$$

In the case of  $\Gamma_A = \Gamma_B = \gamma_\alpha P_L$ , performing the projection  $G$  amounts to replacing  $\otimes$  by  $\gamma_\tau$  on both sides of the above equation and contracting the indices using  $D$ -dimensional Dirac algebra. In this manner, the coefficient  $\xi$  is determined. One finds for instance:

$$G\left[(\bar{s}^\alpha \gamma_\mu \gamma_\nu \gamma_\rho P_L d^\beta)(\bar{u}^\beta \gamma^\mu \gamma^\nu \gamma^\rho P_L c^\alpha)\right] = (16 - 4\epsilon) G\left[Q_1^{\text{VLL}}\right] + \mathcal{O}(\epsilon^2) \quad (\text{D.3})$$

with  $Q_1^{\text{VLL}}$  as defined in eq. (3.1).

It has been pointed out in ref. [5] that for a proper treatment of counterterms in two-loop calculations, one has to use eq. (D.3) only as a prescription for defining an evanescent operator. In the case at hand, this is the operator  $E_1^{\text{VLL}}$  of appendix B. As discussed in ref. [2], in the case of VLR and SLR operators, the analogous projections are performed by replacing  $\otimes$  by 1 and  $\gamma_\tau$ , respectively. Examples of the corresponding evanescent operators can be found in appendices A–C.

The projections in the SLL sector are slightly more involved. In the case of the insertion of  $Q_1^{\text{SLL}}$  or  $Q_3^{\text{SLL}}$ , the r.h.s. of eq. (D.2) has to be generalized to a linear combination of these two operators. The same applies to the pair  $(Q_2^{\text{SLL}}, Q_4^{\text{SLL}})$ . The projection  $G$  is now performed by replacing  $\otimes$  by  $\gamma_\alpha \gamma_\beta$ . After the projection, one finds linear combinations of  $g_{\alpha\beta}$  and  $\gamma_\alpha \gamma_\beta$  on both sides of the equation. This allows extracting the coefficients in question. One finds for instance

$$G\left[(\bar{s}^\alpha \gamma_\mu \gamma_\nu \gamma_\rho \gamma_\sigma P_L d^\beta)(\bar{u}^\beta \gamma^\mu \gamma^\nu \gamma^\rho \gamma^\sigma P_L c^\alpha)\right] = (64 - 96\epsilon) G\left[Q_1^{\text{SLL}}\right] + (16 - 8\epsilon) G\left[Q_3^{\text{SLL}}\right] + \mathcal{O}(\epsilon^2). \quad (\text{D.4})$$

The corresponding evanescent operator is  $E_1^{\text{SLL}}$  in appendix B. An alternative approach to projections can be found in ref. [11].

## Appendix E

In this appendix, the  $1/\epsilon$  and  $1/\epsilon^2$  poles in the one- and two-loop diagrams are given for the  $\Delta F = 1$  calculation in the SLL sector. Analogous results for the remaining sectors can be found in refs. [5] and [6]. The gauge-fixing parameter  $\lambda$  is set to unity here, i.e. the Feynman–’t Hooft gauge is used.

Each insertion results in a linear combination of  $Q_1^{\text{SLL}}, \dots, Q_4^{\text{SLL}}$ , after subtracting the evanescent counterterms (see appendix B) or, alternatively, after performing the ‘‘Greek projections’’ (see appendix D). Table 1 gives the singularities (without colour factors) in the coefficients of the resulting operators, for each diagram separately. The numbering of the diagrams and values of the colour factors are exactly as in figs. 1, 2 and tables 1, 2 of ref. [5]. The multiplicity factors of the diagrams are included.

In the two-loop case, the singularities include one-loop diagrams with counterterm insertions. The counterterms proportional to evanescent operators are multiplied by an additional factor  $1/2$ , and, at the same time, the term  $-2\hat{b}\hat{c}$  in eq. (2.14) is ignored. Correctness of such a trick has been justified in refs. [5, 10].

The singularities from table 1 apply for the pair  $(Q_2^{\text{SLL}}, Q_4^{\text{SLL}})$ , too. After including colour factors and summing the diagrams, the  $1/\epsilon$  singularities build a  $4 \times 4$  matrix in the basis  $\{Q_1^{\text{SLL}}, Q_2^{\text{SLL}}, Q_3^{\text{SLL}}, Q_4^{\text{SLL}}\}$

$$\hat{B} = \frac{\alpha_s}{4\pi} \hat{B}_1 + \left(\frac{\alpha_s}{4\pi}\right)^2 \hat{B}_2 + \mathcal{O}(\alpha_s^3), \quad (\text{E.5})$$

from which the anomalous-dimension matrix can be obtained by means of

$$\gamma_{ij}^{(0)\text{SLL}} = -2 \left[ 2 a_1 \delta_{ij} + (\hat{B}_1)_{ij} \right], \quad (\text{E.6})$$

$$\gamma_{ij}^{(1)\text{SLL}} = -4 \left[ 2 a_2 \delta_{ij} + (\hat{B}_2)_{ij} \right]. \quad (\text{E.7})$$

Here,  $a_1$  and  $a_2$  originate from  $1/\epsilon$  singularities in the quark field renormalization constants. They read

$$a_1 = -C_F, \quad a_2 = C_F \left[ \frac{3}{4} C_F - \frac{17}{4} N + \frac{1}{2} f \right]. \quad (\text{E.8})$$

Remembering the trick applied to evanescent operators here, it is easy to verify that eqs. (E.6) and (E.7) are equivalent to eqs. (2.13) and (2.14) from section 2.

		$Q_1^{\text{SLL}}$				$Q_3^{\text{SLL}}$			
$D$	$M$	$Q_1^{\text{SLL}}$ and $Q_2^{\text{SLL}}$		$Q_3^{\text{SLL}}$ and $Q_4^{\text{SLL}}$		$Q_1^{\text{SLL}}$ and $Q_2^{\text{SLL}}$		$Q_3^{\text{SLL}}$ and $Q_4^{\text{SLL}}$	
		$1/\epsilon^2$	$1/\epsilon$	$1/\epsilon^2$	$1/\epsilon$	$1/\epsilon^2$	$1/\epsilon$	$1/\epsilon^2$	$1/\epsilon$
1	2	–	8	–	0	–	0	–	0
2	2	–	–2	–	–1/2	–	–24	–	–6
3	2	–	2	–	–1/2	–	–24	–	6
4	2	–16	16	0	0	0	0	0	0
5	2	–4	9	–1	5/4	–48	76	–12	7
6	2	–4	9	1	–7/4	48	–52	–12	7
7	2	0	–4	0	0	0	0	0	4
8	2	0	2	0	–1/2	0	–24	0	–2
9	2	0	2	0	1/2	0	24	0	–2
10	4	–8	–8	0	0	0	0	0	4
11	4	2	0	1/2	5/4	24	20	6	8
12	4	–2	0	1/2	5/4	24	20	–6	–4
13	4	8	–4	0	0	0	0	0	0
14	4	–2	0	–1/2	–1/4	–24	28	–6	0
15	4	2	0	–1/2	–1/4	–24	28	6	–4
16	4	8	–4	0	0	96	64	0	0
17	4	8	4	2	2	0	0	0	0
18	4	–8	4	0	0	96	64	0	0
19	4	–8	–4	2	2	0	0	0	0
20	4	–4	10	–1	1	48	–64	12	2
21	4	–4	10	1	–2	–48	112	12	–22
22	1	–16	0	0	0	0	0	0	0
23	1	–4	5	–1	1/4	–48	28	–12	–5
24	1	–4	5	1	–3/4	48	–4	–12	–5
25	4	24	–20	0	0	0	0	0	0
26	4	–6	2	–3/2	–1/4	–72	108	–18	6
27	4	6	–2	–3/2	–1/4	–72	108	18	–18
28	4	0	0	0	3	0	–144	0	0
29	2	$–5N + 2f$	$\frac{26N}{3} - \frac{8f}{3}$	0	0	0	0	$\frac{5N}{3} - \frac{2f}{3}$	$-\frac{16N}{9} + \frac{4f}{9}$
30	2	0	0	$\frac{5N}{12} - \frac{f}{6}$	$-\frac{17N}{72} + \frac{f}{36}$	$20N - 8f$	$-\frac{134N}{3} + \frac{44f}{3}$	$\frac{10N}{3} - \frac{4f}{3}$	$-\frac{32N}{9} + \frac{8f}{9}$
31	2	0	0	$\frac{5N}{12} - \frac{f}{6}$	$-\frac{17N}{72} + \frac{f}{36}$	$20N - 8f$	$-\frac{134N}{3} + \frac{44f}{3}$	$-\frac{10N}{3} + \frac{4f}{3}$	$\frac{62N}{9} - \frac{20f}{9}$

Table 1: Pole parts of the one- and two-loop diagrams with insertions of  $Q_1^{\text{SLL}}$  and  $Q_3^{\text{SLL}}$ . The colour factors are omitted, whereas the multiplicity ( $M$ ) is taken into account. The numbering is according to fig. 2 of ref. [5]. While the singularities in front of the resulting  $Q_1^{\text{SLL}}$  and  $Q_2^{\text{SLL}}$  are the same in this table, they become different after the inclusion of colour factors. The same comment applies to  $Q_3^{\text{SLL}}$  and  $Q_4^{\text{SLL}}$ . When the colour factors are omitted, the results for  $Q_2^{\text{SLL}}$  and  $Q_4^{\text{SLL}}$  insertions are equal to those for  $Q_1^{\text{SLL}}$  and  $Q_3^{\text{SLL}}$  insertions, respectively.

## Appendix F

In the present appendix, we outline details of our determination of the penguin-diagram generated ADMs in eqs. (4.8) and (4.9). Let us begin with the SM QCD-penguin operators  $Q_3, \dots, Q_6$  that are listed in eq. (4.1). Their  $4 \times 4$  ADM can be split into contributions from the current-current and penguin diagrams:  $\hat{\gamma}^{\text{SM}} = \hat{\gamma}_{cc}^{\text{SM}} + \hat{\gamma}_p^{\text{SM}}$ . The structure of  $Q_3, \dots, Q_6$  implies that

$$\hat{\gamma}_{cc}^{\text{SM}} = \begin{pmatrix} \gamma_{22}^{\text{VLL}} & \gamma_{21}^{\text{VLL}} & 0 & 0 \\ \gamma_{12}^{\text{VLL}} & \gamma_{11}^{\text{VLL}} & 0 & 0 \\ 0 & 0 & \gamma_{22}^{\text{VLR}} & \gamma_{21}^{\text{VLR}} \\ 0 & 0 & \gamma_{12}^{\text{VLR}} & \gamma_{11}^{\text{VLR}} \end{pmatrix}, \quad (\text{F.9})$$

where  $\hat{\gamma}^{\text{VLL}}$  and  $\hat{\gamma}^{\text{VLR}}$  up to the two-loop level are given in eqs. (3.2)–(3.5). The matrix  $\hat{\gamma}_p^{\text{SM}}$  is most easily found by subtracting  $\hat{\gamma}_{cc}^{\text{SM}}$  from the full  $\hat{\gamma}^{\text{SM}}$ . One- and two-loop contributions to the latter matrix in the NDR- $\overline{\text{MS}}$  are listed in table 5 of ref. [6].<sup>4</sup> This way one finds

$$\begin{aligned} \hat{\gamma}_p^{\text{SM}(0)} &= \left( \frac{4}{3}, \frac{2f}{3}, 0, \frac{2f}{3} \right)^T \times \left( -\frac{1}{N}, 1, -\frac{1}{N}, 1 \right), \\ \hat{\gamma}_p^{\text{SM}(1)} &= \begin{pmatrix} -\frac{64}{27} + \frac{172}{27N^2} & -\frac{460}{27N} + \frac{352N}{27} & -\frac{244}{27} - \frac{188}{27N^2} & \frac{260}{27N} + \frac{172N}{27} \\ -\frac{4}{3N} + 6N & -\frac{14}{3} & \frac{32}{3N} - 6N & -\frac{14}{3} \\ 0 & 0 & 0 & 0 \\ 0 & 0 & 0 & 0 \end{pmatrix} \\ &+ \begin{pmatrix} -\frac{8}{3N} + 3N & -\frac{1}{3} & \frac{10}{3N} - 3N & -\frac{1}{3} \\ -\frac{20}{27} + \frac{74}{27N^2} & -\frac{164}{27N} + \frac{110N}{27} & -\frac{56}{27} + \frac{2}{27N^2} & -\frac{20}{27N} + \frac{74N}{27} \\ \frac{20}{3N} - 3N & -\frac{11}{3} & \frac{2}{3N} + 3N & -\frac{11}{3} \\ -\frac{56}{27} - \frac{178}{27N^2} & \frac{250}{27N} - \frac{16N}{27} & \frac{70}{27} + \frac{74}{27N^2} & -\frac{254}{27N} + \frac{110N}{27} \end{pmatrix} f. \quad (\text{F.10}) \end{aligned}$$

Let us now extend the considered operator set to  $\{Q_3, Q_4, Q_5, Q_6, Q_{11}, Q'_{11}, Q_{13}, Q_{12}\}$ , where the extra operators have been defined in eqs. (4.2) and (4.6). At this point, we ignore the fact that  $Q_{11}$  and  $Q'_{11}$  are related by a Fierz relation in  $D = 4$ , i.e. we treat both of them as independent normal (non-evanescent) operators.

The four extra operators  $\{Q_{11}, Q'_{11}, Q_{13}, Q_{12}\}$  can be obtained from  $\{Q_3, Q_4, Q_5, Q_6\}$  by skipping the  $u$ -,  $c$ - and  $b$ -quarks in the sum over flavours. Consequently, the full  $8 \times 8$  ADM up to

<sup>4</sup>They coincide with results of independent calculations in refs. [7] and [8].

two loops takes the form

$$\hat{\gamma}_{8 \times 8} = \begin{pmatrix} \hat{\gamma}^{\text{SM}} & 0_{4 \times 4} \\ \hat{\gamma}_{p,f=2}^{\text{SM}} & \hat{\gamma}_{cc}^{\text{SM}} \end{pmatrix}. \quad (\text{F.11})$$

We have tacitly assumed here that each of our operators is accompanied by a corresponding one-loop evanescent operator containing triple products of Dirac matrices inside the quark currents, defined in full analogy to  $E_1^{\text{VLL}}$ ,  $E_2^{\text{VLL}}$ ,  $E_1^{\text{VLR}}$  and  $E_2^{\text{VLR}}$  in appendix B, including the coefficients at the  $\mathcal{O}(\epsilon)$  terms there.

In the next step, we transform our  $8 \times 8$  ADM to the basis  $\{Q_3, Q_4, Q_5, Q_6, Q_{11}, Q_{12}, Q_{13}, E_{11}\}$ , where  $E_{11} = Q'_{11} - Q_{11}$  is still treated as a normal (non-evanescent) operator. The transformed ADM reads

$$\hat{\gamma}'_{8 \times 8} = \hat{R} \hat{\gamma}_{8 \times 8} \hat{R}^{-1} \quad \text{with} \quad \hat{R} = \begin{pmatrix} 1_{4 \times 4} & 0_{4 \times 4} \\ 0_{4 \times 4} & X_{4 \times 4} \end{pmatrix} \quad \text{and} \quad X_{4 \times 4} = \begin{pmatrix} 1 & 0 & 0 & 0 \\ 0 & 0 & 0 & 1 \\ 0 & 0 & 1 & 0 \\ -1 & 1 & 0 & 0 \end{pmatrix}. \quad (\text{F.12})$$

Finally, we depart from the MS scheme for  $E_{11}$  (still thinking of it as of a normal operator though) by introducing finite terms in the one-loop renormalization constants that correspond to its mixing via penguin diagrams into  $Q_3, \dots, Q_6$ . This amounts to replacing  $a_{ik}^{11}$  in eq. (2.15) by  $a_{ik}^{11} + \epsilon a_{ik}^{01}$  when the index  $i$  corresponds to  $E_{11}$ , and the index  $k$  corresponds to  $Q_3, \dots, Q_6$ . We adjust

$$a_{E_{11}, Q_3}^{01} = a_{E_{11}, Q_5}^{01} = -\frac{2}{3N} \quad \text{and} \quad a_{E_{11}, Q_4}^{01} = a_{E_{11}, Q_6}^{01} = \frac{2}{3} \quad (\text{F.13})$$

to make the renormalized one-loop penguin matrix element of  $E_{11}$  vanish. The one-loop ADM remains intact, while the resulting transformation of the two-loop ADM reads (c.f. eq. (6.10))

$$\hat{\gamma}''_{8 \times 8}{}^{(1)} = \hat{\gamma}'_{8 \times 8}{}^{(1)} + [\Delta \hat{r}, \hat{\gamma}'_{8 \times 8}{}^{(0)}] + 2\beta_0 \Delta \hat{r} \quad \text{with} \quad (\Delta r)_{ij} = \delta_{i8} \left[ -\frac{2}{3N} (\delta_{j1} + \delta_{j3}) + \frac{2}{3} (\delta_{j2} + \delta_{j4}) \right]. \quad (\text{F.14})$$

At this point, our non-MS scheme with  $E_{11}$  treated as a normal operator becomes equivalent to the MS scheme with  $E_{11}$  treated as an evanescent operator.<sup>5</sup> We explicitly verify that the 8th row of  $\hat{\gamma}''_{8 \times 8}$  up to two loops has only a single non-vanishing entry that corresponds to the

---

<sup>5</sup>Strictly speaking, this is true only up to finite renormalization in the one-loop mixing of evanescent operators among themselves, which should be absent in the MS scheme. However, such a finite renormalization has no effect on the ADM of the physical operators up to two loops.

mixing of  $E_{11}$  with itself. Consequently, the Wilson coefficient of  $E_{11}$  has no effect on the RG evolution of the Wilson coefficients of normal operators, as it should be for any evanescent operator in the MS scheme. Let us note that it would not be the case if the transformation (F.14) was not performed.

To find the actual ADM for the normal operators only (now with  $E_{11}$  treated as an evanescent operator, and in the MS scheme), we remove the 8th row and 8th column from the matrix  $\hat{\gamma}''_{8 \times 8}$ . The resulting  $7 \times 7$  matrix reads

$$\hat{\gamma}_{7 \times 7} = \begin{pmatrix} \hat{\gamma}^{\text{SM}} & 0_{4 \times 3} \\ \hat{\gamma}_p & \hat{\gamma}_{cc} \end{pmatrix}, \quad (\text{F.15})$$

where the one- and two-loop contributions to  $\hat{\gamma}^{\text{SM}}$ ,  $\hat{\gamma}_{cc}$  and  $\hat{\gamma}_p$  coincide with what has been already given in eqs. (F.9)-(F.10), (4.7) and (4.8)-(4.9), respectively. Our final results for  $\hat{\gamma}_p$  in eqs. (4.8)-(4.9) have actually been extracted from eq. (F.15). As far as  $\hat{\gamma}_{cc}$  in eq. (4.7) is concerned, eq. (F.15) gives us a nice confirmation of the result that has in practice been determined using a much simpler method.

The transformation (F.14) was missed in the original version of our paper in 2000. The mistake was pointed out in ref. [23]. The current appendix was added in 2024, simultaneously with implementing the proper correction in eq. (4.9).

The reader might wonder why our finite subtraction in eq. (F.13) was restricted to the penguin matrix elements only, i.e. why no similar operation was necessary for the one-loop current-current matrix element of  $E_{11}$ . It was the case because such a matrix element turns to vanish after subtracting the evanescent counterterms only, and passing to  $D = 4$ , as already discussed in section 6, below eq. (6.18).

## References

- [1] G. Buchalla, A.J. Buras, M.E. Lautenbacher, *Rev. Mod. Phys.* **68** (1996) 1125.
- [2] A.J. Buras, hep-ph/9806471, in “Probing the Standard Model of Particle Interactions”, eds. R. Gupta, A. Morel, E. de Rafael and F. David, Elsevier Science, Amsterdam 1999, p. 281.
- [3] F. Gabbiani, E. Gabrielli, A. Masiero and L. Silvestrini, *Nucl. Phys.* **B477** (1996) 321.

- [4] M. Ciuchini, E. Franco, V. Lubicz, G. Martinelli, I. Scimemi and L. Silvestrini, Nucl. Phys. **B523** (1998) 501.
- [5] A.J. Buras and P.H. Weisz, Nucl. Phys. **B333** (1990) 66.
- [6] A.J. Buras, M. Jamin, M.E. Lautenbacher and P.H. Weisz, Nucl. Phys. **B400** (1993) 37.
- [7] M. Ciuchini, E. Franco, G. Martinelli and L. Reina, Nucl. Phys. **B415** (1994) 403.
- [8] K. Chetyrkin, M. Misiak and M. Münz, Nucl. Phys. **B520** (1998) 279.
- [9] D. Becirevic et al., hep-lat/0002025 and references therein.
- [10] M. J. Dugan and B. Grinstein, Phys. Lett. **B256** (1991) 239.
- [11] S. Herrlich and U. Nierste, Nucl. Phys. **B455** (1995) 39.
- [12] K. Chetyrkin, M. Misiak and M. Münz, Nucl. Phys. **B518** (1998) 473.
- [13] A.J. Buras, M. Jamin and P.H. Weisz, Nucl. Phys. **B347** (1990) 491.
- [14] A.J. Buras, M. Jamin M.E. Lautenbacher and P.H. Weisz, Nucl. Phys. **B370** (1992) 69; addendum Nucl. Phys. **B375** (1992) 501.
- [15] G. Altarelli and L. Maiani, Phys. Lett. **B52** (1974) 351.
- [16] M.K. Gaillard and B.W. Lee, Phys. Rev. Lett. **33** (1974) 108.
- [17] A.I.Vainshtein, V.I. Zakharov and M.A. Shifman, Sov. Phys. JETP **45** (1977) 670.
- [18] F.J. Gilman and M.B. Wise, Phys. Rev. **D20** (1979) 2392.
- [19] B. Guberina and R.D. Peccei, Nucl. Phys. **B163** (1980) 289.
- [20] J.A. Bagger, K.T. Matchev and R.J. Zhang, Phys. Lett. **B412** (1997) 77.
- [21] G. Altarelli, G. Curci, G. Martinelli and S. Petrarca, Nucl. Phys. **B187** (1981) 461.
- [22] N. Tracas and N. Vlachos, Phys. Lett. **B115** (1982) 419.
- [23] P. Morell and J. Virto, arXiv:2402.00249.